

State-Specific Coupled-Cluster Methods for Excited States

Yann Damour,* Anthony Scemama, Denis Jacquemin, Fábri Kossoski,* and Pierre-François Loos*

Cite This: *J. Chem. Theory Comput.* 2024, 20, 4129–4145

Read Online

ACCESS |



Metrics & More

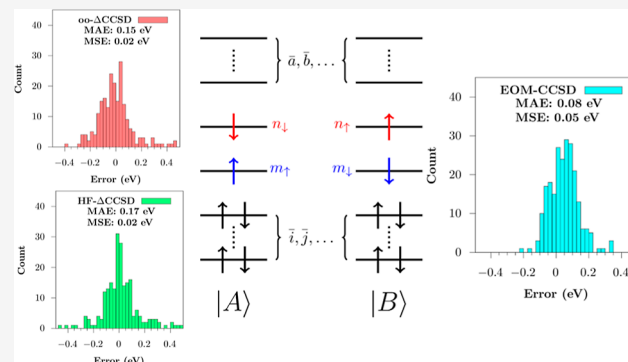


Article Recommendations



Supporting Information

ABSTRACT: We reexamine Δ CCSD, a state-specific coupled-cluster (CC) with single and double excitations (CCSD) approach that targets excited states through the utilization of non-Aufbau determinants. This methodology is particularly efficient when dealing with doubly excited states, a domain in which the standard equation-of-motion CCSD (EOM-CCSD) formalism falls short. Our goal here to evaluate the effectiveness of Δ CCSD when applied to other types of excited states, comparing its consistency and accuracy with EOM-CCSD. To this end, we report a benchmark on excitation energies computed with the Δ CCSD and EOM-CCSD methods for a set of molecular excited-state energies that encompasses not only doubly excited states but also doublet–doublet transitions and (singlet and triplet) singly excited states of closed-shell systems. In the latter case, we rely on a minimalist version of multireference CC known as the two-determinant CCSD method to compute the excited states. Our data set, consisting of 276 excited states stemming from the QUEST database [Vénil et al., *WIREs Comput. Mol. Sci.* 2021, 11, e1517], provides a significant base to draw general conclusions concerning the accuracy of Δ CCSD. Except for the doubly excited states, we found that Δ CCSD underperforms EOM-CCSD. For doublet–doublet transitions, the difference between the mean absolute errors (MAEs) of the two methodologies (of 0.10 and 0.07 eV) is less pronounced than that obtained for singly excited states of closed-shell systems (MAEs of 0.15 and 0.08 eV). This discrepancy is largely attributed to a greater number of excited states in the latter set exhibiting multiconfigurational characters, which are more challenging for Δ CCSD. We also found typically small improvements by employing state-specific optimized orbitals.



1. INTRODUCTION

Over the past few years, significant advances have been made toward the accurate description of molecular excited states, with a particular emphasis on vertical excitation energies from the electronic ground state. These advances have been realized by solving the Schrödinger equation in the basis of many-electron functions using a set of judicious and appropriate approximations. In such a way, numerous innovative methods have emerged, each characterized by distinct strategies designed to describe the ground and excited states.^{1–11}

The prominent density-functional theory (DFT)^{12–15} provides a framework to study electronic excited states through time-dependent DFT,^{16–19} by applying the linear-response formalism on top of a ground-state calculation. Similarly, single-reference coupled-cluster (SRCC)^{20–25} methods compute excitation energies based on the ground-state amplitudes. This is done by either constructing and diagonalizing the similarity-transformed Hamiltonian in equation-of-motion coupled-cluster (EOM-CC)^{26–32} or by examining the poles of the linear-response function in linear-response coupled-cluster (LRCC).^{28,33–36} Consequently, the excited states provided by these frameworks are inherently biased toward the ground state upon which they are built. As a direct consequence, even if EOM- and LR-CC are, in principle, exact,

the accuracy of such approaches is known to be quite poor for certain classes of excited states where the truncation of the excitation operator is too severe compared to the degree of the excitation. This is typically the case for doubly excited states when EOM/LR-CC is restricted to single and double excitations.^{37–42}

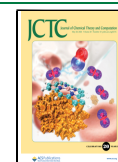
Nevertheless, other strategies can be used with different methods to address this limitation. In configuration interaction (CI),⁴³ excited-state energies are obtained through the diagonalization of the Hamiltonian matrix within a basis of Slater determinants. However, since the results are highly dependent on the underlying orbitals, their choice is critical. To deal with this issue, the states can be treated in a state-averaged approach, i.e., using the same set of orbitals for the states of interest, thereby treating them on an equal footing.^{44,45} Excitation energies can then be straightforwardly extracted as energy differences between these states.

Received: January 10, 2024

Revised: March 6, 2024

Accepted: March 6, 2024

Published: May 15, 2024



Alternatively, one can employ a state-specific approach, which requires the use of orbitals optimally designed for each of the states of interest and implies separate calculations for each of them. When seeking to evaluate the excitation energy between two states, it is intuitive to expect the state-specific approach to yield more accurate results. Nonetheless, certain issues might be encountered, such as keeping track of the targeted state because of possible root-flipping.^{46,47} Similarly, variational collapse may happen while trying to follow the potential energy surface of a given excited state. Thus, even if such problems can occur, by adopting one of these two approaches (state-averaged or state-specific), the calculations are no longer subject to an orbital-related bias toward the ground state.

At the self-consistent-field (SCF) level, such as Hartree–Fock (HF) or DFT, the well-known Δ SCF method employs non-Aufbau determinants with orbitals that are optimized in a state-specific manner to describe excited states.^{48–50} A considerable body of research has been dedicated to the Δ SCF family of methods, yielding promising results, notably for doubly excited and charge-transfer states.^{51–66} Multi-reference self-consistent-field^{67–72} and multireference perturbation theory^{73–78} methods have also been extensively applied in a state-averaged or state-specific way.^{59,79–83} In particular, some of us have recently employed a state-specific CI approach applied to a vast number and various classes of excited states.⁸⁴ Finally, selected configuration interaction (SCI) methods^{85–112} are known for their ability to provide results approaching full CI (FCI) quality, though they are usually restricted to relatively small systems and basis sets.

Similar studies have been undertaken in the context of CC theory. Notably, the work of Lee et al. showed that the Δ CC approach can provide accurate excitation energies for both doubly excited and double-core-hole states.¹¹³ Mayhall and Raghavachari achieved something similar a decade earlier when they successfully converged multiple coupled-cluster with singles and doubles (CCSD) solutions for the NiH molecule.¹¹⁴ Other works reported the use of Δ CC,^{115,116} notably for processes implying core excitations.^{117–123} This methodology has also been exploited by Schraivogel and Kats within the distinguishable cluster approximation^{124,125} yielding promising results in the case of open-shell systems as well as excited states.¹²⁶ This kind of approach has been also applied for low-order and cheaper CC methods such as pair coupled-cluster doubles.^{116,127,128}

All of these works have been inspired by the discovery of multiple CC solutions. Živković and Monkhorst were the first to study the conditions under which higher roots of the CC equations exist,^{129,130} while Adamowicz and Bartlett explored the feasibility of reaching certain excited states of the LiH molecule.¹³¹ Subsequently, Jankowski et al. clearly evidenced that some of these nonstandard CC solutions are unphysical.^{132–134} A pivotal development in the study of nonstandard CC solutions was the introduction of the homotopy method¹³⁵ by Kowalski, Jankowski, and others.^{136–143} We refer the interested reader to the review of Piecuch and Kowalski for additional information on this topic¹⁴⁴ (see also refs 145–148. for a more mathematical perspective).

Unfortunately, some electronic states require multireference treatment to efficiently achieve an accurate description of their electronic structure. A simple example is the singly excited state of a closed-shell molecule, which must be described by at least two determinants related by a global spin-flip transformation, forming a single configuration state function (CSF).

Within the CI formalism, a multireference treatment is relatively straightforward as it only requires designing an appropriate reference before applying excitations.^{149,150} However, on the CC side, the situation is considerably more complex and implies the use of multireference CC (MRCC) methods. To avoid this, Tuckman and Neuscamman recently proposed an alternative way to deal with open-shell singlet excited states within the SRCC formalism.^{151,152}

MRCC methods have been a center of interest since the inception of SRCC methods despite the various challenges they present. Interested readers can find reviews on this topic elsewhere.^{24,153–156} In MRCC, the wave function is constructed through the application of a wave operator to a model wave function composed of multiple Slater determinants. MRCC methods can be separated into two main categories, namely, Fock-space MRCC (FS-MRCC),^{157–165} also known as valence-universal MRCC (VU-MRCC), and Hilbert-space MRCC (HS-MRCC).^{166–178} The primary distinction between these two categories lies in their respective configuration spaces. FS-MRCC computes states within the Fock space, i.e., with a variable number of electrons. In contrast, HS-MRCC considers only determinants within a specified Hilbert space, i.e., with a fixed number of electrons. Methods based on the HS-MRCC can be designed in several manners. In the state-universal (SU) formalism,^{179,180} one considers multiple electronic states, while the single-root or state-specific formalism looks at each state separately.^{168,175–177,181–183} The intermediate Hamiltonian formalism leads to a restricted number of relevant states among all the computed roots.^{164,165,184–188}

One common challenge encountered with multistate approaches is the potential emergence of intruder states. However, an interesting observation is that the open-shell singlet and triplet states that are correctly described by two determinants can be effectively treated with the SU-MRCC approach using an incomplete active space (IAS-SU-MRCC) containing only the two determinants of interest. The resulting scheme is then free of the intruder state problem. Moreover, while the use of the Jeziorski–Monkhorst ansatz in SU-MRCC usually requires solving simultaneous equations for all the references,^{166,169} in this particular case, the equations are considerably simplified due to the spin-flip relationship between the two reference determinants. It leads to the so-called two-determinant CC (TD-CC) approach developed by Bartlett's group.^{170,172,189–192} Likewise, Piecuch and co-workers have formulated a spin-adapted version of TD-CC.^{193–199}

In this paper, we employ state-specific CCSD and TD-CCSD to consistently treat various classes of excited states. The vertical excitation energies are computed within the Δ CCSD framework and subsequently compared with EOM-CCSD and state-of-the-art high-order EOM-CC or extrapolated FCI (exFCI) calculations. Both ground-state HF and state-specific orbitals are employed to build the reference, chosen as a single- or two-determinant wave function, depending on the targeted state, as discussed in detail below. Our main goal of this work is to assess the performance of state-specific CC methods to describe different types of excited states. The present manuscript is organized as follows. Section 2 recalls the working equations of SRCC and MRCC. It also quickly explains how one can compute excitation energies within the different formalisms. Section 3 presents the computational details, while Section 4 discusses the main

results and compares the performance of the state-specific approach with that of the standard EOM-CCSD method. Our conclusions are drawn in Section 5.

2. THEORY

2.1. Single-Reference Coupled Cluster. In CC theory, the wave function is expressed as an exponential ansatz

$$|\Psi\rangle = e^{\hat{T}}|\Phi_0\rangle \quad (1)$$

where an excitation operator

$$\hat{T} = \sum_{n=1}^N \hat{T}_n \quad (2)$$

is exponentiated and applied on a reference determinant $|\Phi_0\rangle$ to create new determinants. The excitation operator is composed of a sum of n -electron operators

$$\hat{T}_n = (n!)^{-2} \sum_{ij\cdots} \sum_{ab\cdots} t_{ij\cdots}^{ab\cdots} \hat{a}_a^\dagger \hat{a}_b^\dagger \cdots \hat{a}_j \hat{a}_i \quad (3)$$

associated with cluster amplitudes $t_{ij\cdots}^{ab\cdots}$ that promote n electrons from occupied spin orbitals (ϕ_i, ϕ_j, \dots) in $|\Phi_0\rangle$, to virtual spin orbitals (ϕ_a, ϕ_b, \dots) using respectively annihilation (\hat{a}) and creation (\hat{a}^\dagger) second-quantized operators. For the sake of simplicity, we shall use the following shortcut notations: $\hat{p}^\dagger \equiv \hat{a}_p^\dagger$ and $\hat{p} \equiv \hat{a}_p$.

The equations for the energy and the amplitudes are determined using the time-independent Schrödinger equation

$$\hat{H}|\Psi\rangle = E|\Psi\rangle \quad (4)$$

by projecting on either $\langle\Phi_0|e^{-\hat{T}}$ for the energy

$$\langle\Phi_0|\bar{H}|\Phi_0\rangle = E \quad (5)$$

or $\langle\Phi_{ij\cdots}^{ab\cdots}|e^{-\hat{T}}$ for the amplitudes

$$\langle\Phi_{ij\cdots}^{ab\cdots}|\bar{H}|\Phi_0\rangle = 0 \quad (6)$$

where $\langle\Phi_{ij\cdots}^{ab\cdots}| = \langle\Phi_0|\hat{i}^\dagger \hat{j}^\dagger \cdots \hat{b} \hat{a}$ is an excited determinant and $\bar{H} = e^{-\hat{T}} \hat{H} e^{\hat{T}}$ is the (non-Hermitian) similarity-transformed Hamiltonian. To ensure that the number of unknown amplitudes matches the number of equations, the latter equation must be solved for all of the excited determinants that can be built from the application of \hat{T} on $|\Phi_0\rangle$.

The second-quantized form of the Hamiltonian operator mentioned in the previous equations is

$$\hat{H} = \sum_{pq} \langle\phi_p|\hat{h}|\phi_q\rangle \hat{p}^\dagger \hat{q} + \frac{1}{4} \sum_{pqrs} \langle\phi_p \phi_q || \phi_r \phi_s\rangle \hat{p}^\dagger \hat{q}^\dagger \hat{s} \hat{r} \quad (7)$$

where p, q, r , and s are general indices that run over all spin orbitals ($\phi_i \phi_j \cdots \phi_a \phi_b \cdots$), $\langle\phi_p|\hat{h}|\phi_q\rangle$ are the elements of the core Hamiltonian and $\langle\phi_p \phi_q || \phi_r \phi_s\rangle$ are the antisymmetrized two-electron integrals. It is convenient to define the normal-ordered Hamiltonian

$$\hat{H}_N = \sum_{pq} \langle\phi_p|\hat{f}|\phi_q\rangle \{\hat{p}^\dagger \hat{q}\} + \frac{1}{4} \sum_{pqrs} \langle\phi_p \phi_q || \phi_r \phi_s\rangle \{\hat{p}^\dagger \hat{q}^\dagger \hat{s} \hat{r}\} \quad (8)$$

where $\{\cdots\}$ means that the second-quantized operators inside the curly brackets are normal-ordered with respect to the

Fermi vacuum Φ_0 and $\langle\phi_p|\hat{f}|\phi_q\rangle$ are the elements of the Fock matrix. More detailed explanations about normal ordering and CC theory can be found elsewhere.^{23,25}

2.2. Equation-of-Motion Coupled Cluster. In CC theory, excited states can be accessed via the EOM^{26–32} and LR^{28,33–36} formalisms. Both frameworks yield identical excitation energies but result in different molecular properties.^{24,112,200,201} In the following subsection, we provide a brief overview of EOM-CC to emphasize the distinctions between this approach and its state-specific counterpart, discussed later.

In EOM-CC, one seeks to solve the following modified Schrödinger equation

$$\hat{H}_N |\Psi^{(k)}\rangle = \Delta E^{(k)} |\Psi^{(k)}\rangle \quad (9)$$

where $|\Psi^{(k)}\rangle$ is the k th excited state of energy $E^{(k)}$, $\Delta E^{(k)} = E^{(k)} - E_0$, and E_0 is the energy of the reference wave function. This excited state is created from the CC ground-state wave function

$$|\Psi^{(0)}\rangle = e^{\hat{T}}|\Phi_0\rangle \quad (10)$$

of energy $E^{(0)}$ by applying a linear excitation operator $\hat{R}^{(k)}$, such that

$$|\Psi^{(k)}\rangle = \hat{R}^{(k)} |\Psi^{(0)}\rangle \quad (11)$$

with

$$\hat{R}^{(k)} = r_0 + \sum_{n=1}^N \hat{R}_n^{(k)} \quad (12)$$

$$\hat{R}_n^{(k)} = (n!)^{-2} \sum_{ij\cdots} \sum_{ab\cdots} r_{ij\cdots}^{ab\cdots} \hat{a}_a^\dagger \hat{a}_b^\dagger \cdots \hat{a}_j \hat{a}_i \quad (13)$$

where $r_{ij\cdots}^{ab\cdots}$ are the EOM right amplitudes. Hence, by multiplying the left-hand side of eq 9 by $e^{-\hat{T}}$ and rearranging the equation, one gets

$$\bar{H}_N \hat{R}^{(k)} |\Phi_0\rangle = \Delta E^{(k)} \hat{R}^{(k)} |\Phi_0\rangle \quad (14)$$

where $\bar{H}_N = e^{-\hat{T}} \hat{H}_N e^{\hat{T}}$ is the normal-ordered version of the similarity-transformed Hamiltonian. Because the matrix representation of \bar{H}_N and \hat{H}_N share, in the limit of a complete basis, the same spectrum of eigenenergies, the diagonalization of \bar{H}_N within a suitable basis of Slater determinants yields the energies $\Delta E^{(k)}$ and the corresponding eigenvectors $\hat{R}^{(k)} |\Phi_0\rangle$. Note that, because \bar{H} is non-Hermitian, two sets of biorthogonal eigenvectors can be obtained, usually referred to as the right and left eigenvectors, and denoted, respectively, as $\hat{R}^{(k)} |\Phi_0\rangle$ and $\langle\Phi_0|\hat{L}^{(k)}$, respectively, where $\hat{L}^{(k)}$ is a linear de-excitation operator. Additional details can be found elsewhere.^{23,25}

2.3. Multi-Reference Coupled Cluster. Within the MRCC formalism, one seeks a wave operator $\hat{\Omega}$, which creates the exact wave function $|\Psi\rangle$ when applied to a model wave function $|\Psi_0\rangle$, i.e.

$$|\Psi\rangle = \hat{\Omega} |\Psi_0\rangle \quad (15)$$

and fulfills the so-called Bloch equation

$$\hat{H} \hat{\Omega} = \hat{\Omega} \hat{H} \hat{\Omega} \quad (16)$$

The model wave function, which lives in the model space \mathcal{M}_0 , is built as a linear combination of determinants $|I\rangle$ associated with coefficients c_I , as follows

$$|\Psi_0\rangle = \sum_{I \in \mathcal{M}_0} c_I |I\rangle \quad (17)$$

From this, one can define a projector operator onto \mathcal{M}_0

$$\hat{P} = \sum_{I \in \mathcal{M}_0} \hat{P}_I = \sum_{I \in \mathcal{M}_0} |I\rangle\langle I| \quad (18)$$

For the sake of simplicity, we assume that Ψ_0 is normalized and we adopt the intermediate normalization between Ψ_0 and Ψ , i.e., $\langle \Psi_0 | \Psi_0 \rangle = 1$ and $\langle \Psi_0 | \Psi \rangle = 1$.

The key strength of this multireference formalism appears when eq 15 is plugged into the Schrödinger equation and subsequently multiplied by \hat{P} on the left-hand side, which yields

$$\hat{P} \hat{H} \hat{\Omega} \hat{P} |\Psi_0\rangle = E |\Psi_0\rangle \quad (19)$$

because $\hat{P} \hat{\Omega} = \hat{\Omega} \hat{P} = \hat{P}$ and $\hat{P} |\Psi_0\rangle = |\Psi_0\rangle$. Thus, it can be rewritten as

$$\hat{H}^{\text{eff}} |\Psi_0\rangle = E |\Psi_0\rangle \quad (20)$$

meaning that the eigenvalues of \hat{H} can be obtained by only diagonalizing the effective Hamiltonian

$$\hat{H}^{\text{eff}} = \hat{P} \hat{H} \hat{\Omega} \hat{P} \quad (21)$$

which has the size of the model space \mathcal{M}_0 . As TD-CC is based on HS-MRCC, we briefly review the latter in Section 2.4. The interested reader can find additional details about MRCC (including its Fock-space variant) elsewhere.^{25,154}

2.4. Hilbert-Space MRCC. In Hilbert-space MRCC, one considers the Jeziorski–Monkhorst form of the wave operator,¹⁶⁶ which reads

$$\hat{\Omega} = \sum_{I \in \mathcal{M}_0} e^{I\hat{T}} \hat{P}_I \quad (22)$$

where $I\hat{T}$ is a cluster operator defined for the reference I that contains restrictions to remove all the excitations within the model space.

The amplitude equations related to each determinant within the model space are obtained by recasting the previous expression into the Bloch eq 16, projecting onto a determinant within the model space $|A\rangle$ and a determinant outside the model space $\langle A_{ij}^{ab} |$

$$\langle A_{ij}^{ab} | \hat{H} e^{A\hat{T}} | A \rangle - \sum_{I \in \mathcal{M}_0} \langle A_{ij}^{ab} | e^{I\hat{T}} | I \rangle \langle I | \hat{H} e^{A\hat{T}} | A \rangle = 0 \quad (23)$$

where $H_{IA}^{\text{eff}} = \langle I | \hat{H} e^{A\hat{T}} | A \rangle$ are the matrix elements of the effective Hamiltonian defined in eq 21.

These amplitude equations must be solved simultaneously for all references A within the model space. As the matrix elements H_{IA}^{eff} depend on reference-dependent amplitudes $A\hat{T}$, they must be updated, at each iteration, after the computation of the new amplitudes. Nonetheless, in the special case where the model space is restricted to only two determinants related by a global spin-flip transformation, one ends up with the TD-

CC equations that require only one set of amplitudes to be solved. We explore this special case in Section 2.5.

2.5. Two-Determinant Coupled Cluster. In TD-CC, the reference space is built from two open-shell determinants, $|A\rangle$ and $|B\rangle$, related by a global spin-flip transformation

$$|A\rangle = \hat{n}_\downarrow^\dagger \hat{m}_\uparrow^\dagger |\Phi_{\text{core}}\rangle |B\rangle = \hat{n}_\uparrow^\dagger \hat{m}_\downarrow^\dagger |\Phi_{\text{core}}\rangle \quad (24)$$

where Φ_{core} is a closed-shell determinant containing the common doubly occupied orbitals of A and B . These determinants are represented in Figure 1, where the labels

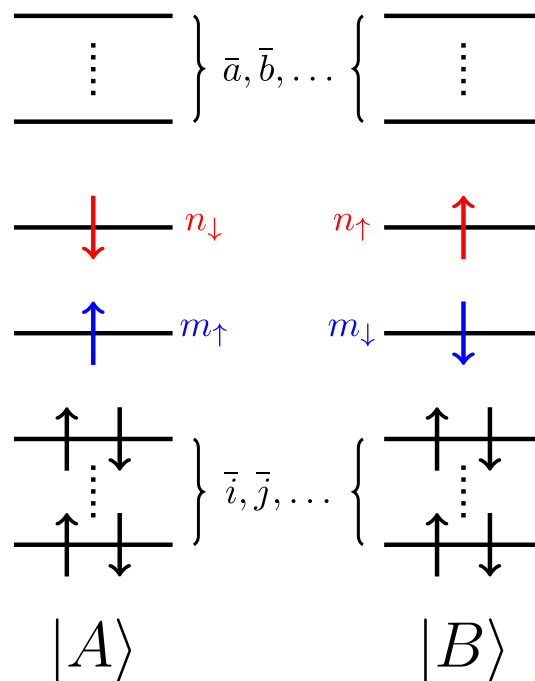


Figure 1. Occupancy of the two reference determinants in TD-CC, $|A\rangle$ and $|B\rangle$, which are related by a global spin-flip transformation.

corresponding to the different classes of orbitals are specified: \bar{i}, \bar{j}, \dots for doubly occupied orbitals, m or n for active or singly occupied orbitals, and \bar{a}, \bar{b}, \dots for virtual orbitals. Thus, in the following, occupied and virtual spin orbitals are labeled i, j, \dots and a, b, \dots , respectively. For the reference $|A\rangle$, we have

$$\{i, j, \dots\} = \{\bar{i}, \bar{j}, \dots\} \cup \{m_\uparrow, n_\downarrow\} \quad (25a)$$

$$\{a, b, \dots\} = \{\bar{a}, \bar{b}, \dots\} \cup \{m_\downarrow, n_\uparrow\} \quad (25b)$$

and likewise for the reference $|B\rangle$

$$\{i, j, \dots\} = \{\bar{i}, \bar{j}, \dots\} \cup \{m_\downarrow, n_\uparrow\} \quad (26a)$$

$$\{a, b, \dots\} = \{\bar{a}, \bar{b}, \dots\} \cup \{m_\uparrow, n_\downarrow\} \quad (26b)$$

The model space is thus composed of one singlet (S) and one triplet (T) model wave function

$$|^S\Psi_0\rangle = \frac{|A\rangle + |B\rangle}{\sqrt{2}} \quad |^T\Psi_0\rangle = \frac{|A\rangle - |B\rangle}{\sqrt{2}} \quad (27)$$

Thus, using eqs 15 and 22, the TDCC singlet and triplet wave functions are

$$|{}^S\Psi\rangle = \frac{e^{A_T}|A\rangle + e^{B_T}|B\rangle}{\sqrt{2}} \quad |{}^T\Psi\rangle = \frac{e^{A_T}|A\rangle - e^{B_T}|B\rangle}{\sqrt{2}} \quad (28)$$

Because of the spin-flip relation between these model wave functions, the diagonalization of the effective Hamiltonian leads to the following energies for the singlet and triplet states

$$E^S = \langle A|\hat{H}_N e^{A_T}|A\rangle + \langle A|\hat{H}_N e^{B_T}|B\rangle \quad (29a)$$

$$E^T = \langle A|\hat{H}_N e^{A_T}|A\rangle - \langle A|\hat{H}_N e^{B_T}|B\rangle \quad (29b)$$

At the TD-CCSD level, the excitation operators are restricted to single and double excitations with respect to their respective references. For example, we have

$$\begin{aligned} \hat{T}^A &= \hat{T}_1^A + \hat{T}_2^A \\ &= \sum_{ia} A_{ti}^a \hat{a}^\dagger \hat{t}_i + \frac{1}{4} \sum_{ijab} A_{tij}^{ab} \hat{a}^\dagger \hat{b}^\dagger \hat{t}_j \hat{t}_i \end{aligned} \quad (30)$$

with a similar expression for the reference *B*. Note that excitations of the form $t_{m_1 n_1}^{m_1} \hat{m}_1^\dagger \hat{n}_1^\dagger \hat{t}_1 \hat{m}_1$, which link $|A\rangle$ to $|B\rangle$, are removed from the summation since the excitations between two determinants of the active space must be discarded.

The A_{T_1} equations for the reference-dependent amplitudes are

$$\begin{aligned} A_{T_1}^a &= \langle A_i|\hat{H}_N e^{A_T}|A\rangle_c - (\langle A_i|\hat{H}_N e^{B_T}|B\rangle H_{BA}^{\text{eff}})_c \\ &= \langle A_i|\hat{H}_N e^{A_T}|A\rangle_c - A_{M_i}^a H_{BA}^{\text{eff}} = 0 \end{aligned} \quad (31)$$

while, for the A_{T_2} equations, we have

$$\begin{aligned} A_{T_2}^{ab} &= \langle A_{ij}|\hat{H}_N e^{A_T}|A\rangle_c - (\langle A_{ij}|\hat{H}_N e^{B_T}|B\rangle H_{BA}^{\text{eff}})_c \\ &\quad - P(ij, ab)[(\hat{A}_{ti}^a - \hat{R}_{ia} \hat{B}_{ti}^a)(\langle A_j|\hat{H}_N e^{B_T}|B\rangle H_{BA}^{\text{eff}})_c] \\ &= \langle A_{ij}|\hat{H}_N e^{A_T}|A\rangle_c - A_{M_{ij}}^{ab} H_{BA}^{\text{eff}} = 0 \end{aligned} \quad (32)$$

where \hat{H}_N is normal-ordered with respect to *A*, M_i^a , and M_{ij}^{ab} are the so-called renormalization terms, the subscript *c* indicates that only connected terms are considered, $\hat{R}_{ia} = (1 - \delta_{in_1})(1 - \delta_{im_1})(1 - \delta_{am_1})(1 - \delta_{an_1})$, and $P(ij, ab) = 1 - (i \leftrightarrow j) - (a \leftrightarrow b) + (i \leftrightarrow j)(a \leftrightarrow b)$ is a permutation operator. It is worth noting that one only needs to solve eqs 31 and 32 for the reference *A* since the corresponding amplitudes for *B* can be easily obtained thanks to the global spin-flip relationship between *A* and *B*. Further explanations and explicit expressions of each quantity can be found in refs 172, 191, and 192.

Furthermore, as explained by Lutz et al.,¹⁹² only two out of four determinants contribute to the singlet and triplet states in the case of a complete active space (CAS) containing two electrons in two orbitals of different spatial symmetries (as for H_2 in a minimal basis set). Therefore, TD-CC is performed on top of a (2,2) complete active space, and the CC single excitation amplitudes between the active orbitals are zero, further simplifying the equations. However, in the case where the active space contains two orbitals of the same spatial symmetry, TD-CC accounts for an incomplete active space.

The working equations for both scenarios are presented in the Supporting Information.

2.6. Derivation of the TD-CCSD Equations. The TD-CCSD equations can be derived by hand using Wick's theorem or diagrammatic techniques.¹⁶⁹ However, the manual manipulation of a substantial number of equations and indices is highly prone to errors, especially during their implementation in computer software. Fortunately, software solutions are available to streamline this process. Notably, tools such as $p^\dagger q$ by Rubin and DePrince²⁶² and WICK&D developed by Evangelista²⁰³ can algebraically derive this kind of equations in various contexts.

Let us take a look at eq 31 for the A_{T_1} amplitudes. The first term in the right-hand-side of eq 31, $\langle A_i|\hat{H}_N e^{A_T}|A\rangle_c$, corresponds to the standard term of the T_1 SRCC equations considered in eq 6, with a restriction over the summations in A_{T_1} . The only new part is the renormalization term, $(\langle A_i|\hat{H}_N e^{B_T}|B\rangle H_{BA}^{\text{eff}})_c$. To compute the latter term, it is convenient to express each component with respect to a unique reference. For example, the term $H_{BA}^{\text{eff}} = \langle B|\hat{H} e^{A_T}|A\rangle$ can be obtained by rewriting $|B\rangle$ as an excitation from $|A\rangle$ using eq 24, i.e.

$$\begin{aligned} |B\rangle &= \hat{n}_1^\dagger \hat{m}_1^\dagger |\Phi_{\text{core}}\rangle \\ &= \hat{n}_1^\dagger \hat{m}_1^\dagger \hat{m}_1 \hat{n}_1 \hat{n}_1^\dagger \hat{m}_1^\dagger |\Phi_{\text{core}}\rangle \\ &= \hat{n}_1^\dagger \hat{m}_1^\dagger \hat{n}_1 \hat{m}_1 |A\rangle \\ &= |A_{n_1 m_1}^{n_1 m_1}\rangle \end{aligned} \quad (33)$$

Thus, the quantity that needs to be evaluated is $\langle A_{n_1 m_1}^{n_1 m_1}|\hat{H} e^{A_T}|A\rangle$, which is simply one of the SRCC T_2 equations with additional restrictions over the summations in A_{T_1} .

The derivation of the second part of the renormalization term, $M_i^a = \langle A_i|\hat{H} e^{B_T}|B\rangle$, is a little bit more involved. Due to the presence of $e^{B_T}|B\rangle$, it is easier to express $\langle A_i|$ as an excitation from the reference $|B\rangle$. To do so, we start by rewriting $|A\rangle$ as an excitation from $|B\rangle$

$$\begin{aligned} |A\rangle &= \hat{n}_1^\dagger \hat{m}_1^\dagger |\Phi_{\text{core}}\rangle \\ &= \hat{n}_1^\dagger \hat{m}_1^\dagger \hat{m}_1 \hat{n}_1 \hat{n}_1^\dagger \hat{m}_1^\dagger |\Phi_{\text{core}}\rangle \\ &= \hat{n}_1^\dagger \hat{m}_1^\dagger \hat{n}_1 \hat{m}_1 |B\rangle \end{aligned} \quad (34)$$

which yields

$$|A_i^a\rangle = \hat{a}^\dagger \hat{i} \hat{n}_1^\dagger \hat{m}_1^\dagger \hat{m}_1 \hat{n}_1 |B\rangle \quad (35)$$

At this stage, a difficulty arises from the fact that *A* and *B* do not share the same set of occupied and virtual spin orbitals because of the two unpaired electrons, as shown in Figure 1 and eqs 25a, 26a, 25b, and 26b. To solve this issue, we generate a set of strings of second-quantized operators corresponding to every possible combination of occupancy and spin cases and apply them to $|B\rangle$

$$(\hat{a}_o^\dagger \hat{n}_\downarrow^\dagger \hat{m}_\uparrow^\dagger \hat{m}_\downarrow^\dagger \hat{n}_\uparrow^\dagger)^\dagger \rightarrow \{(\hat{a}_o^\dagger \hat{i}_o^\dagger \hat{n}_\downarrow^\dagger \hat{m}_\uparrow^\dagger \hat{m}_\downarrow^\dagger \hat{n}_\uparrow^\dagger)^\dagger, (\hat{a}_v^\dagger \hat{i}_o^\dagger \hat{n}_\downarrow^\dagger \hat{m}_\uparrow^\dagger \hat{m}_\downarrow^\dagger \hat{n}_\uparrow^\dagger)^\dagger, (\hat{a}_o^\dagger \hat{i}_v^\dagger \hat{n}_\downarrow^\dagger \hat{m}_\uparrow^\dagger \hat{m}_\downarrow^\dagger \hat{n}_\uparrow^\dagger)^\dagger, (\hat{a}_v^\dagger \hat{i}_v^\dagger \hat{n}_\downarrow^\dagger \hat{m}_\uparrow^\dagger \hat{m}_\downarrow^\dagger \hat{n}_\uparrow^\dagger)^\dagger\} \quad (36)$$

where the subscripts *o* (occupied) and *v* (virtual) specify the occupancy of the spin orbitals of reference *A* in the reference *B*. Note that we have not specified the spin of ϕ_a and ϕ_i on purpose to reduce the number of terms. Otherwise, by including their spin, each string would lead to four additional terms, that is, $\uparrow\uparrow$, $\uparrow\downarrow$, $\downarrow\uparrow$, and $\downarrow\downarrow$. Subsequently, Wick's theorem is applied to each of the generated strings. The result is a set of normal-ordered strings of second-quantized operators with Kronecker deltas.

To avoid errors, we have implemented Wick's theorem for a single string of second-quantized operators in Python. The source code is freely available on github at <https://github.com/LCPQ/SimpleWick> and archived in the SOFTWARE HERITAGE database.²⁰⁴ As a reminder, Wick's theorem is a technique to rewrite an arbitrary string of second-quantized operators into a sum of normal-order strings.^{23,25,205} Thus, to evaluate

$${}^A M_i^a = \langle A_i^a | e^{\hat{T}} | B \rangle = \langle B | (\hat{a}_o^\dagger \hat{i}_\downarrow^\dagger \hat{m}_\uparrow^\dagger \hat{m}_\downarrow^\dagger \hat{n}_\uparrow^\dagger)^\dagger e^{\hat{T}} | B \rangle \quad (37)$$

the string $(\hat{a}_o^\dagger \hat{i}_\downarrow^\dagger \hat{m}_\uparrow^\dagger \hat{m}_\downarrow^\dagger \hat{n}_\uparrow^\dagger)^\dagger$ is expanded and evaluated as explained above. The resulting strings of normal-ordered second-quantized operators are reordered and fed to $p^\dagger q$ as left operators of the form $\{\hat{i}^\dagger \hat{j}^\dagger \dots \hat{b} \hat{a}\}$ using the occupancy definition of eqs 26a and 26b, to be separately evaluated. Schematically, we evaluate terms of the form

$$\langle B | \{\hat{i}^\dagger \hat{j}^\dagger \dots \hat{b} \hat{a}\} e^{\hat{T}} | B \rangle \quad (38)$$

The use of Wick's theorem allows us to handle the different occupancy cases. To illustrate this, let us consider the first term of eq 36 that contributes to ${}^A M_{i_1}^{a_1}$. In this case, we have

$$\hat{n}_\uparrow^\dagger \hat{m}_\downarrow^\dagger \hat{m}_\uparrow^\dagger \hat{n}_\downarrow^\dagger \hat{i}_o^\dagger \hat{a}_o^\dagger = \{\hat{n}_\uparrow^\dagger \hat{m}_\downarrow^\dagger \hat{m}_\uparrow^\dagger \hat{n}_\downarrow^\dagger \hat{i}_o^\dagger \hat{a}_o^\dagger\} + \delta_{na} \{\hat{m}_\downarrow^\dagger \hat{m}_\uparrow^\dagger \hat{n}_\downarrow^\dagger \hat{i}_o^\dagger\} \quad (39)$$

Obviously, the contraction between *a* and *i*, as well as the contraction between *n* and *m*, are zero since they correspond to distinct spin orbitals. In addition, it is straightforward to see that the first term of the previous equation yields a zero contribution. Thus, we have

$${}^A M_{i_1}^{a_1} = \delta_{na} \langle B | \{\hat{m}_\downarrow^\dagger \hat{i}_o^\dagger \hat{m}_\uparrow^\dagger \hat{n}_\downarrow^\dagger\} e^{\hat{T}} | B \rangle \quad (40)$$

which becomes

$$\begin{aligned} {}^A M_{i_1}^{n_1} &= {}^B t_{m_1 i_1}^{n_1 m_1} + {}^B t_{m_1}^{n_1} {}^B t_{i_1}^{m_1} \\ &= {}^A t_{m_1 i_1}^{n_1 m_1} + {}^A t_{m_1}^{n_1} {}^A t_{i_1}^{m_1} \end{aligned} \quad (41)$$

However, because our aim is to evaluate $(\langle A_i^a | e^{\hat{T}} | B \rangle H_{BA}^{\text{eff}})_c$, we must remove the disconnected contributions. To do so, the terms involving at least one cluster amplitude not connected to the effective Hamiltonian, i.e., a cluster amplitude that does not contain any active label, like *m* or *n*, are excluded. Then, the generated terms are associated with the Kronecker deltas and

the signs coming from Wick's theorem. At this stage, all quantities are related to reference *B*. We thus perform a global spin-flip transformation on M_i^a to express the latter quantity with respect to reference *A*. Finally, the contributions to M_i^a are generated for computer implementation. A similar procedure is applied to the renormalization term of the ${}^A T_2$ equations [see eq 32].

To perform all of these tasks, we have developed a Python code that interfaces $p^\dagger q$ with the Wick theorem code described above. It enables to generate LaTeX formulas and Fortran code with ease within a jupyter notebook. This code is also freely available on github at https://github.com/LCPQ/Gen_Eq_TDCC, and archived in the SOFTWARE HERITAGE database.²⁰⁶ For the sake of completeness, the automatically derived formulas related to eqs 31 and 32 can be found in the Supporting Information.

3. COMPUTATIONAL DETAILS

Most of the molecules and states considered in this paper have been studied in ref 84 and were originally extracted from the quest database.²⁰⁷ The geometries are also taken from the quest database while the state-specific orbitals are the same as those of ref 84 (see below). We employ the aug-cc-pVDZ basis set for molecules with three or fewer non-hydrogen atoms and the 6-31+G(d) basis otherwise, applying the frozen core approximation (large core for third-row atoms). In the special case of the Be atom, the aug-cc-pVDZ basis set was chosen so as to comply with ref 208. Furthermore, we rely on the same reference values as in ref 84, which are mainly of CC with singles, doubles, triples, and quadruples (CCSDTQ) or exFCI quality. We consider two new systems, borole and oxalyl fluoride, with geometries optimized at the CC3/aug-cc-pVTZ level of theory following the QUEST methodology. These are reported in the Supporting Information.

Our set of excited states comprises 125 singlet, 36 doublet, and 106 triplet states in small- and medium-sized organic compounds, among which there are 9 doubly excited states. Compared to ref 84, a few states were removed for reasons detailed below.

In this paper, all the calculations were performed with the QUANTUM PACKAGE software,⁹⁹ where CCSD (for both open- and closed-shell systems) and TD-CCSD have been implemented. The calculations were carried out by using the Δ CC strategy. Hence, the excitation energies from the ground state were straightforwardly determined as the energy difference between ground and excited states. The ground-state energies were computed with the CCSD and ground-state HF orbitals. Different strategies were applied to compute excited states based on their nature. For doubly excited states, a CCSD calculation was performed on top of a closed-shell doubly excited determinant. Similarly, for the doublet excited states, a CCSD calculation was performed on top of a singly excited determinant. Finally, for open-shell singlet and triplet excited states, a TD-CCSD calculation was undertaken by using a pair of open-shell singly excited determinants as the reference.

Concerning the choice of the orbitals, we employ both the ground-state HF and the state-specific optimized orbitals. At the HF level, we rely systematically on the restricted HF and restricted open-shell HF (ROHF) formalisms for closed- and open-shell systems, respectively. The state-specific orbitals, extracted from our recent work,⁸⁴ were obtained by optimizing the orbitals for a minimal CSF space using the Newton–Raphson method, also implemented in the quantum pack-

Table 1. Excitation Energies Associated with the Doubly Excited States Calculated at Various Levels of Theory^a

molecule	% T_1 ^b	excitation energies eV					
		ref.	Δ SCF	HF- Δ CCSD ^c	oo- Δ CCSD	EOM-CC3	EOM-CCSDT
beryllium	29	7.22	7.86(+0.64)	7.23(+0.01)	7.23(+0.01)	7.23(+0.01)	7.22(+0.00)
borole	20	4.71	5.70(+0.99)	5.16(+0.45)	5.33(+0.62)	5.41(+0.70)	5.07(+0.36)
ethylene	20	13.07	13.54(+0.47)	13.10(+0.03)	13.31(+0.24)	13.57(+0.50)	13.20(+0.13)
formaldehyde	5	10.45	10.83(+0.38)		10.53(+0.08)	11.22(+0.77)	10.78(+0.33)
glyoxal	0	5.60	10.50(+4.90)	6.67(+1.07)	6.55(+0.95)	6.74(+1.14)	6.24(+0.64)
nitrosomethane	3	4.84	4.96(+0.12)	5.06(+0.22)	5.07(+0.23)	5.75(+0.91)	5.26(+0.42)
nitroxyl	0	4.40	4.57(+0.17)	4.65(+0.25)	4.66(+0.26)	5.25(+0.85)	4.76(+0.36)
oxalyl fluoride	2	9.21	12.57(+3.37)	10.30(+1.09)	10.16(+0.95)	10.26(+1.05)	9.86(+0.66)
tetrazine	1	5.06	7.77(+2.71)	5.36(+0.30)	5.58(+0.52)	6.22(+1.16)	5.86(+0.79)

^aThe error with respect to the reference value is reported in parentheses. ^bPercentage of single excitations involved in the transition computed at the CC3/aug-cc-pVTZ level. ^cFor formaldehyde, we were unable to locate unambiguously the electronic state of interest at this level of theory.

age.^{99,106} We refer to HF- Δ CCSD as a Δ CCSD calculation where ground-state HF orbitals have been considered for both ground and excited states, while oo- Δ CCSD denotes a Δ CCSD calculation that employs HF orbitals for the ground state and state-specific optimized orbitals for the excited state. For HF- Δ CCSD, excited-state calculations were performed by changing the orbital occupancy to match with the excited-state dominant determinant obtained from a prior EOM-CCSD calculation. For oo- Δ CCSD, excited-state calculations were done for a non-Aufbau single CSF reference for which the orbitals were optimized. It is important to note that the orbitals in oo- Δ CCSD are optimized for a single CSF wave function. In other words, they do not minimize the CCSD energy as in orbital-optimized CCSD.^{209–212}

In the statistical analysis presented below, we report the usual indicators: the mean signed error (MSE), the mean absolute error (MAE), the root-mean-square error (RMSE), and the standard deviation of the errors (SDE). For the sake of completeness, the raw data associated with each figure and table, in addition to the total and excitation energies computed at the different levels of theory, are reported in the [Supporting Information](#).

4. RESULTS AND DISCUSSION

4.1. Doubly Excited States. For the doubly excited states, we limited our focus to a small subset of nine molecules, including the six listed in ref 84, complemented with borole, oxalyl fluoride, and tetrazine. Other molecules such as C_2 and C_3 are excluded from this study since they require consideration of more than one closed-shell determinant to accurately describe their doubly excited states.⁸⁴ This requirement becomes evident when examining the coefficients of their CI wave function. Additionally, we restrict ourselves to “genuine” double excitations only, which have a small contribution from the single excitations (see the % T_1 values in Table 1) and are hence reasonably well described by a single closed-shell determinant. Transitions with a dominant single excitation character, yet a significant partial double excitation contribution (large % T_1 values), such as the famous 2^1A_g dark state of butadiene,^{37–40,42,213} are treated as single excitations using TD-CCSD (see Section 4.3). Most of the reference data for these transitions have been extracted from ref 40.

The results for each system are represented in Figure 2 and are also collected in Table 1, where we further report the Δ SCF results and the value of % T_1 computed at the CC3/aug-cc-pVTZ level. We do not consider EOM-CCSD due to the very poor quality of the results. Indeed, it is well-known

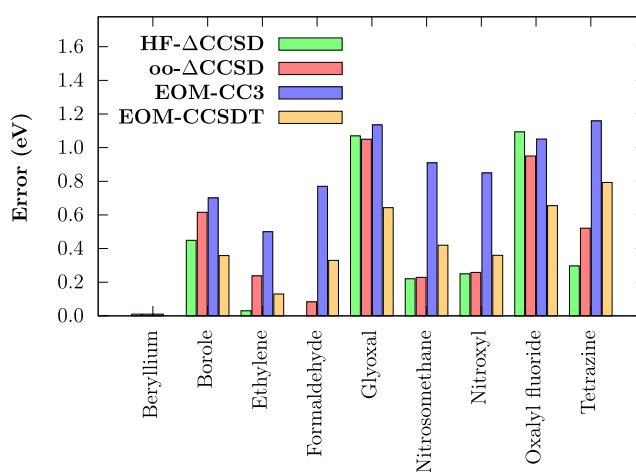


Figure 2. Errors in the excitation energies (with respect to the reference values) of doubly excited states computed at various levels of theory. See Table 1 for the raw data.

that, at this level of theory, some of the doubly excited states are overshot by several eV. For the doubly excited states, we do not perform a statistical analysis due to the limited number of states.

Interestingly, we found that HF- Δ CCSD generally yields results similar to those of oo- Δ CCSD, with the exception of formaldehyde, for which we were not able to locate the state of interest with HF- Δ CCSD. This result reveals a limited effect of mean-field orbital optimization for Δ CCSD calculations. It is also worth noting that both HF- Δ CCSD and oo- Δ CCSD systematically overestimate the excitation energies, hinting at the importance of the missing contributions from higher excitations (see below).

Glyoxal and oxalyl fluoride exhibit the largest errors of our set (around 1 eV), with both HF- Δ CCSD and oo- Δ CCSD. Based on SCI calculations for both molecules and with both methods, we found that the CI coefficient associated with the reference determinant of the excited state is large (≈ 0.8). One possible explanation for the observed discrepancy lies in the existence of a second doubly excited determinant, relative to both the HF and the reference determinant, which carries a substantial weight in the wave function (≈ 0.2). Indeed, for glyoxal, including this second determinant in the reference space leads to improved results in state-specific CI with singles and doubles (Δ CISD) calculations.⁸⁴ It is also interesting to notice that the presence of singly excited determinants with somewhat larger coefficients (up to ≈ 0.3) is problematic,

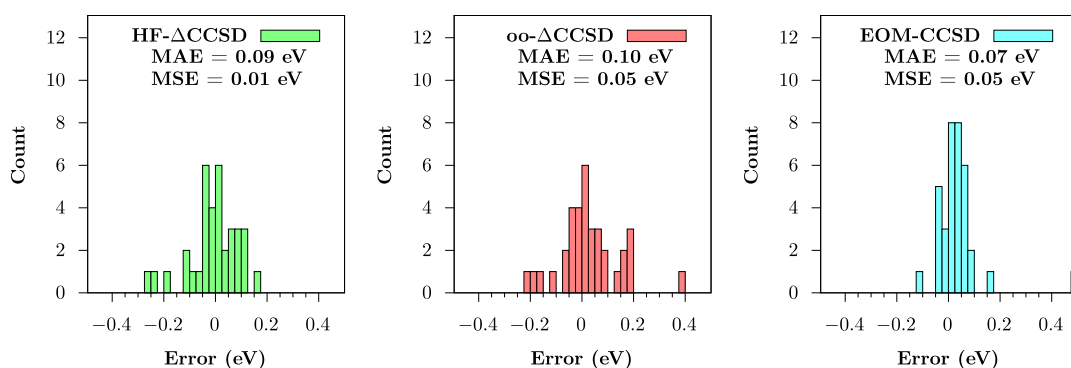


Figure 3. Histograms of the error in excitation energies (with respect to the reference values) computed at the HF-ΔCCSD (left), oo-ΔCCSD (center), and EOM-CCSD (right) levels for doublet–doublet transitions.

based on the smaller errors we observe in the other doubly excited states. Therefore, the inaccuracies for glyoxal and oxalyl fluoride may originate from the fact that important single and double excitations accessed from the second doubly excited determinant are not accounted for, which would appear as triple and quadruple excitations with respect to the reference determinant and are thus lacking in the ΔCCSD calculations. This also explains the systematically overestimated excitation energies.

When compared with standard EOM-CC methods, the ΔCCSD approach demonstrates its superiority for the doubly excited states surveyed here, outperforming EOM-CC3 and even EOM-CCSDT in some cases. However, ΔCCSD becomes less accurate when dealing with systems possessing several doubly excited determinants with significant weights, as discussed above for glyoxal and oxalyl fluoride.

4.2. Doublet–Doublet Transitions. We included all the radical doublets from ref 84, except for 11 states (outlined below), making a total of 36 states in the present set. The reference data for these molecules have been extracted from ref 208. We did not consider the four states of nitromethyl, since their assignment is particularly challenging due to the significant deviations observed between EOM-CCSD and EOM-CCSDT. We also excluded one state of BeH as the two states of interest share the same dominant determinant and one state of BeF, for which we did not manage to converge the orbital optimization. Moreover, HF-ΔCCSD leads to very large errors for two states of CH, as they need two open-shell determinants to be qualitatively described.⁸⁴ Hence, they were also been discarded. Finally, we did not consider one of the states of vinyl and the two states of OH which need three determinants with three unpaired electrons to be described.⁸⁴ The detailed results for all the states can be found in the [Supporting Information](#).

Our set of 36 doublet–doublet transitions should be large enough to render reasonable statistics. The distribution of errors with respect to accurate reference values, as obtained with EOM-CCSD, HF-ΔCCSD, and oo-ΔCCSD, is illustrated in Figure 3, whereas the associated statistical measures are reported in Table 2. When compared with EOM-CCSD, the distribution of errors for HF-ΔCCSD and oo-ΔCCSD appears to be less sharp, leading to slightly worse statistics. Indeed, the distributions are similar for HF-ΔCCSD and oo-ΔCCSD, with comparable MAEs (0.09 to 0.10 eV), both underperforming EOM-CCSD, which has a MAE of 0.07 eV. The same can be concluded from the RMSEs and SDEs. Surprisingly, in contrast to HF-ΔCCSD, which has a near-zero MSE, oo-ΔCCSD has

Table 2. Statistical Indicators Associated with the Errors in Doublet–Doublet Transitions Computed at the EOM-CCSD, HF-ΔCCSD, and oo-ΔCCSD Levels^a

method	# states	MAE	MSE	RMSE	SDE
EOM-CCSD	36	0.07	0.05	0.13	0.12
HF-ΔCCSD	36	0.09	0.01	0.15	0.15
oo-ΔCCSD	36	0.10	0.05	0.17	0.16

^aAll values are given in eV.

the same slightly positive MSE (0.05 eV) as EOM-CCSD. Thus, the use of optimized orbitals instead of HF ground-state orbitals does not improve the overall accuracy. On the contrary, the MAE, RMSE, and SDE are slightly larger (by 0.01 or 0.02 eV) when optimized orbitals are employed, which could be a statistical artifact though. Overall, the accuracy of ΔCCSD for doublet–doublet transitions is only marginally worse compared to that of EOM-CCSD.

We further notice that oo-ΔCCSD is more accurate than the ΔCISD calculations reported in ref 84, with respective MAEs of 0.10 and 0.16 eV. Since both methods employ the same set of state-specific orbitals, reference wave function, and excitation manifold (singles and doubles), the superior performance of oo-ΔCCSD can be attributed to the inclusion of higher-order excitations accessed through the connected terms of CC.

4.3. Open-Shell Singly Excited States. Let us now focus on the performance of the ΔCCSD for open-shell singly excited states of closed-shell systems. Out of the 237 states considered, two could not be targeted with our protocol for HF-ΔCCSD calculations since their dominant determinants are the same as those of a lower-lying excited state. In addition, the HF-TDCC calculations did not converge for four other states, making a total of 231 converged states. All the results are available in the [Supporting Information](#), with the above-mentioned problematic cases highlighted in magenta.

The distribution of errors in the excitation energy for the three methods assessed here is depicted in Figure 4, and the corresponding statistical analysis is reported in Table 3. For the full set of singly excited states, HF-ΔCCSD and oo-ΔCCSD share a near-zero MSE (0.02 eV), and a comparable accuracy, with a small advantage for the latter (MAE of 0.15 eV against 0.17 eV). oo-ΔCCSD produces fewer outliers than HF-ΔCCSD, which is clear from their corresponding RMSEs, of 0.27 and 0.35 eV. oo-ΔCCSD is also more consistent than HF-ΔCCSD, having SDEs of 0.26 and 0.35 eV. Orbital optimization enhances the description of singly excited states,

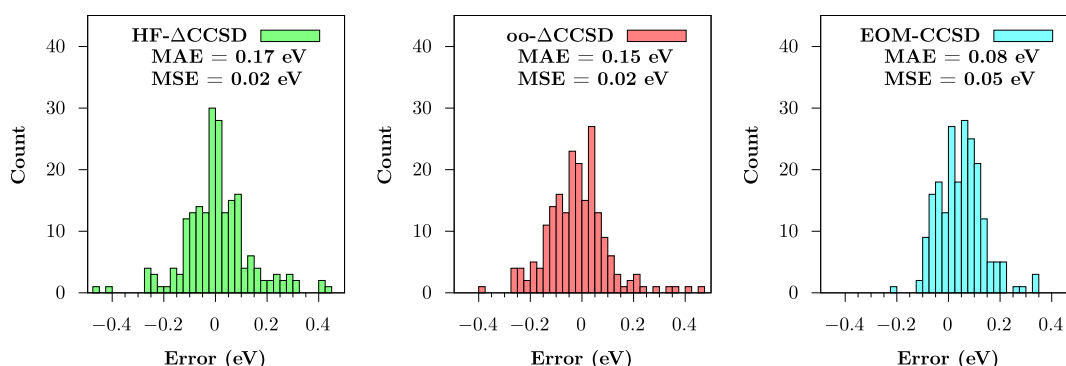


Figure 4. Histograms of the error in excitation energies (with respect to the reference values) at the HF-ΔCCSD (left), oo-ΔCCSD (center), and EOM-CCSD (right) levels for open-shell singly excited states.

Table 3. Statistical Results Associated with the Errors in Excitation Energies (with Respect to the Reference Values) for the Singlet and Triplet Singly Excited States Computed with EOM-CCSD, HF-ΔCCSD, and oo-ΔCCSD^a

method	character	# states	MAE	MSE	RMSE	SDE
EOM-CCSD	all	231 (212)	0.08 (0.09)	0.05 (0.05)	0.13 (0.13)	0.12 (0.12)
	singlet	125 (116)	0.10 (0.10)	0.09 (0.09)	0.13 (0.13)	0.09 (0.10)
	triplet	106 (96)	0.07 (0.06)	−0.01 (−0.00)	0.12 (0.13)	0.12 (0.13)
	valence	152 (133)	0.09 (0.09)	0.04 (0.05)	0.14 (0.14)	0.13 (0.14)
	Rydberg	79 (79)	0.08 (0.08)	0.05 (0.05)	0.09 (0.09)	0.08 (0.08)
HF-ΔCCSD	all	231 (212)	0.17 (0.13)	0.02 (−0.01)	0.35 (0.28)	0.35 (0.28)
	singlet	125 (116)	0.17 (0.11)	0.03 (−0.02)	0.38 (0.29)	0.38 (0.29)
	triplet	106 (96)	0.18 (0.15)	−0.01 (−0.01)	0.32 (0.28)	0.32 (0.28)
	valence	152 (133)	0.20 (0.14)	0.06 (0.02)	0.36 (0.24)	0.35 (0.24)
	Rydberg	79 (79)	0.12 (0.12)	−0.07 (−0.07)	0.34 (0.34)	0.33 (0.33)
oo-ΔCCSD	all	231 (212)	0.15 (0.12)	0.02 (−0.01)	0.27 (0.20)	0.26 (0.20)
	singlet	125 (116)	0.15 (0.11)	0.04 (0.00)	0.29 (0.18)	0.29 (0.18)
	triplet	106 (96)	0.13 (0.12)	−0.00 (−0.03)	0.23 (0.22)	0.23 (0.22)
	valence	152 (133)	0.17 (0.13)	0.04 (−0.02)	0.31 (0.22)	0.31 (0.22)
	Rydberg	79 (79)	0.09 (0.09)	−0.01 (−0.01)	0.15 (0.15)	0.15 (0.15)

^aValues in parentheses are obtained by discarding 19 states having four dominant determinants with the exact same weight in the EOM-CCSD vector, which are all $\pi\pi^*$ valence excitations involving degenerate orbitals. All values are in eV.

particularly for those poorly characterized by HF-ΔCCSD, providing a more accurate overall representation. Both methods compare unfavorably with EOM-CCSD, however, which has a considerably smaller MAE (0.08 eV), RMSE, and SDE, although it shows a somewhat positive MSE (0.05 eV). Compared to the closer performances of HF-ΔCCSD, oo-ΔCCSD, and EOM-CCSD for doublet–doublet transitions, the larger discrepancies for singly excited states are noteworthy.

HF-ΔCCSD and oo-ΔCCSD show a substantial number of absolute errors exceeding 0.2 eV, in contrast to EOM-CCSD. This significantly deteriorates the statistics of these methods since 19 and 15 states, respectively, have errors above 0.5 eV. For EOM-CCSD, this happens for 2 states only. Understanding the reasons behind the inaccuracy of HF-ΔCCSD and oo-ΔCCSD for these specific cases is important. TD-CC is expected to perform well for states described by a single CSF; however, it is less effective for excited states that exhibit pronounced multiconfigurational character, which would necessitate additional CSFs. To evaluate its performance for the former type of states only, we excluded 19 states having four dominant determinants with the exact same weight in the EOM-CCSD vector, which are indicated in red in the [Supporting Information](#). These transitions involve degenerate π/π^* orbitals and require at least two CSFs to be qualitatively

described. The associated statistics excluding results from this subset of singly excited states are shown in parentheses in [Table 3](#). By discarding these multiconfigurational excited states, the statistics for both HF-ΔCCSD and oo-ΔCCSD are systematically improved. In particular, the MAE of HF-ΔCCSD decreases from 0.17 to 0.13 eV, whereas that of oo-ΔCCSD decreases from 0.15 to 0.12 eV. The accuracy of ΔCCSD methods thus approaches that of EOM-CCSD, which remains almost unaltered (with a slightly larger MAE of 0.09 eV) in this case. Moreover, the comparable improvement for both HF-ΔCCSD and oo-ΔCCSD suggests that orbital optimization is overall equally helpful for the single and multiconfigurational excited states.

Further examination of the EOM-CCSD eigenvectors shows that HF-ΔCCSD and oo-ΔCCSD usually deliver larger errors for states with important contributions coming from several determinants, especially when these determinants are doubly excited with respect to the two determinants considered for the TD-CC calculation. From this last point, the magnitude of the errors becomes less surprising since we perform all single and double excitations on top of a two-determinant reference. For instance, by further discarding the three excited states having the largest contribution from doubly excited determinants with respect to those used in TD-CC (based on the EOM-CCSD vector), namely, the 1^3A_1 state of cyclopentadiene, the 2^1B_2

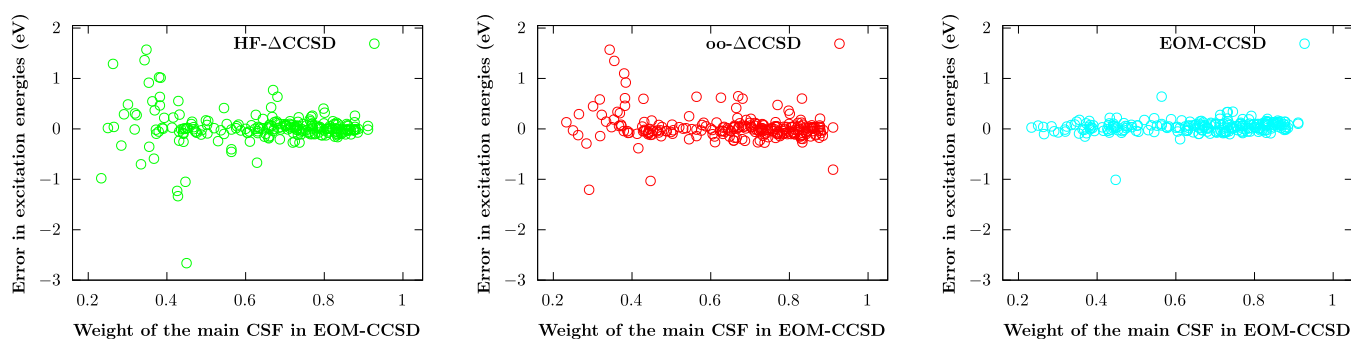


Figure 5. Scatter plots of the error in excitation energies (with respect to reference values) computed at the HF-ΔCCSD (left), oo-ΔCCSD (center), and EOM-CCSD (right) levels for open-shell singly excited states, as functions of the weight, in the EOM-CCSD vector, of the CSF employed as a reference in the TD-CCSD calculation.

state of cyclopropanone, and the 1^3A_g state of butadiene, highlighted in yellow in the [Supporting Information](#), one obtains even smaller MAEs for HF-ΔCCSD and oo-ΔCCSD, of 0.12 and 0.11 eV, whereas the MAE of EOM-CCSD remains unchanged at 0.09 eV. Clearly, the performance of ΔCC methods, TD-CC in particular, approaches the one of EOM-CCSD for states dominated by a single open-shell CSF but deteriorates as the multiconfigurational character of the excited states becomes more pronounced.

The latter point is illustrated in [Figure 5](#), where we inspect the evolution of the excitation energy errors as a function of the weight, in the EOM-CCSD vector, of the CSF employed as a reference in the TD-CCSD calculation. It becomes evident that the accuracy of the excitation energies deteriorates as the weight of the predominant CSF decreases. Similarly, the analysis of the same quantities at the EOM-CCSD level evidence that EOM-CCSD manages to more accurately describe multi-CSF states. Complementarily, if we now look in [Figure 6](#) at the evolution of the MAE of the excitation

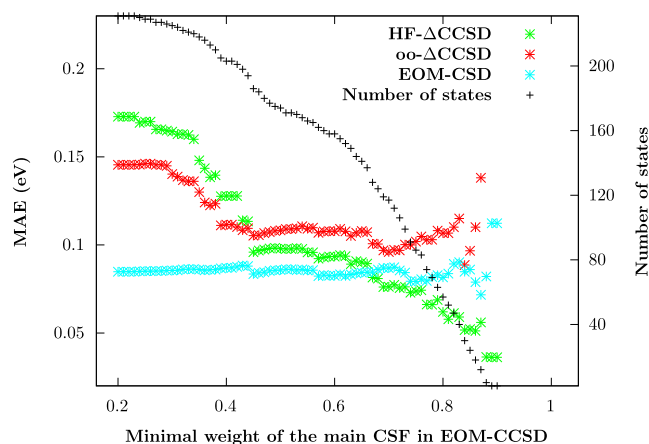


Figure 6. MAE of the excitation energy errors of HF-ΔCCSD, oo-ΔCCSD, and EOM-CCSD, computed on subsets of states for which the predominant CSF employed as a reference in the TD-CCSD calculation has a weight higher than a given value.

energies computed on the subset of states for which the predominant CSF has a weight higher than a given value, we find distinct trends for TD-CCSD and EOM-CCSD. If we keep all the states, TD-CCSD has a large MAE and underperforms EOM-CCSD. If we retain only the states with a weight above 0.45, HF-ΔCCSD and EOM-CCSD exhibit very similar MAEs, while HF-ΔCCSD becomes more accurate

than EOM-CCSD when the weight of the states exceeds 0.67. However, caution is warranted for the final data points where the weight of the primary CSF exceeds 0.85, due to the limited number of states in this region. Consequently, HF-ΔCCSD outperforms EOM-CCSD only for states adequately represented by a single CSF.

In contrast, the performance of the oo-ΔCCSD differs significantly. While it yields lower MAEs than HF-ΔCCSD in the region of low weights, it exhibits minimal improvement as weights increase and never surpasses EOM-CCSD. This discrepancy is likely attributable to the presence of states with substantial excitation energy errors despite a high weight assigned to the considered CSF, as depicted in [Figure 5](#). It may be related to difficulties in targeting the state of interest.

Although the previous trends are likely valid for doublet–doublet transitions, we were unable to draw definitive conclusions due to the limited number of states available for analysis.

Another important aspect concerns the accuracy of the ΔCCSD methods, with respect to the nature of the excitation. As can be seen from [Table 3](#), EOM-CCSD suffers from significant differences in its MAE and MSE when comparing singlet and triplet states. This behavior may be attributed to variations in the $\%T_1$ values, as triplets generally have typically much higher $\%T_1$ than singlets.²⁰⁷ Thus, it is reasonable to expect a more favorable treatment of triplets with EOM-CCSD. On the other hand, HF-ΔCCSD and oo-ΔCCSD share a similar MAE and MSE, meaning that ΔCCSD demonstrates greater consistency in the treatment of singlet and triplet states. When disregarding the more problematic multiconfigurational excited states, the small gap between the MAE for singlets and triplets is preserved in the case of oo-ΔCCSD, but it actually increases for HF-ΔCCSD, becoming comparable to that of EOM-CCSD.

When looking at the statistics for valence and Rydberg states, ΔCCSD seems to be less consistent than EOM-CCSD. While it provides a better treatment of the Rydberg states, the description of the valence states is less satisfactory. The same trend is observed in EOM-CCSD, though to a lesser degree. A closer examination of the statistics reveals that the issue primarily arises from the $\pi\pi^*$ transitions, which are less accurately described than the other valence excitations (the results are shown in the [Supporting Information](#)). However, the gap between valence and Rydberg transitions encountered for ΔCCSD is considerably reduced once the 19 multiconfigurational excited states described above are discarded

(see Table 3). In fact, EOM-CCSD also exhibits a poorer description of $\pi\pi^*$ transitions, albeit by a smaller margin.

oo- Δ CCSD is also more accurate than Δ CISD⁸⁴ for the singly excited states, with respective MAEs of 0.10 and 0.16 eV, respectively. To have a fair comparison, these MAEs were computed by considering the subset of 203 excited states described by a single CSF reference in ref 84. In this case, the two sets of calculations differ only by the connectedness of CC, which implicitly accounts for higher-order excitations. The 0.06 eV improvement equals the one found for the doublet–doublet transitions.

5. CONCLUDING REMARKS

In this work, we studied the use of state-specific CCSD approaches to compute vertical excitation energies and compared them with the standard EOM-CCSD approach. Thanks to the present implementation of TD-CCSD and CCSD based on a non-Aufbau determinant, we conducted a substantial number of calculations on various types of excited states to assess the performance of these state-specific approaches. Our investigation began with closed-shell doubly excited states, where Δ CCSD is known to work quite well (see, for example, ref 113). Next, we extended our exploration to doublet–doublet transitions in radicals, for which both ground and excited states are generally well-described by a single (open-shell) Slater determinant. Finally, we inspected more traditional single excitation processes leading to both singlet and triplet excited states using TD-CCSD, which allows us to perform CCSD calculations on top of a single CSF.

In the context of doubly excited states, Δ CCSD produces results that are comparable to EOM-CCSDT and significantly more accurate than EOM-CCSD. This is an expected outcome because, by construction, at the EOM-CCSD level, the similarity-transformed Hamiltonian only contains the reference determinant in addition to its single and double excitations. This level of description is simply insufficient to accurately describe the genuine doubly excited states considered here, which require the inclusion of triples and quadruples to be properly correlated.

The results for the other kinds of states yielded somewhat unexpected outcomes. Indeed, because EOM-CCSD is biased toward the ground state, one might expect improved results by starting from a more suitable, state-specific reference. However, our findings did not indicate any substantial improvement with the state-specific approaches followed here. Additionally, employing optimized orbitals for the reference CSF in oo- Δ CCSD did not lead to a significant improvement in the accuracy when compared to HF- Δ CCSD. This observation may be attributed to the fact that our optimized orbitals minimize the energy associated with the reference CSF but do not minimize the corresponding CCSD energy. Nonetheless, it is noteworthy that, for most of the states investigated here, Δ CCSD did not significantly deteriorate the quality of the doublet states as compared to EOM-CCSD, with a small MAE increase from 0.07 to 0.10 eV (for oo- Δ CCSD).

Finally, for singlet and triplet singly excited states, Δ CCSD produced twice larger errors (MAEs of 0.15 to 0.17 eV) than EOM-CCSD (MAE of 0.08 eV). Excited states with strong multiconfigurational character are less well described with Δ CCSD approaches, which could be expected. Ignoring the most pathological multireference states from the statistics reduces the MAEs by 0.03 to 0.04 eV, which is however not

enough to match the systematically very good performance of EOM-CCSD for the states considered here. However, we demonstrate that for states characterized by a significant weight on a single CSF, Δ CCSD yields more accurate results than EOM-CCSD. Hence, it is important to note that Δ CCSD is best suited for single-reference problems compared with EOM-CCSD. We also found that state-specifically optimizing the orbitals leads to a small but statistically significant improvement for this class of excitation. On the bright side, Δ CCSD enables a more consistent treatment of singlet and triplet states than EOM-CCSD. Consequently, Δ CCSD may offer an attractive alternative for achieving a more consistent treatment of excited states of different spin multiplicities, which remains to be explored. State-specifically optimizing the ground- and excited-state orbitals at the CCSD level is another avenue one should explore but is left as a future work.

In comparison to standard multiconfigurational methods, such as CASPT2 or NEVPT2, Δ CCSD demonstrates an interesting performance. While the former methods typically yield excitation energy errors in the range of 0.1 to 0.2 eV^{78,214–216} and involve a computational complexity that grows factorially with the size of the active space, Δ CCSD provides excitation energies with errors between 0.10 and 0.15 eV at a computational cost scaling polynomially with the system size. Thus, Δ CCSD may emerge as an appealing alternative for accurately describing excitations that demand a large active space in multiconfigurational methods.

In addition to the classes of excited states considered in the present benchmark study, there remains the unexplored class of charge-transfer states, which could be of particular interest for future assessments of Δ CCSD.^{217,218} In this case, orbital relaxation is known to be crucial,⁶⁶ and thus Δ CCSD may be expected to outperform EOM-CCSD. In addition, the present analysis mainly focused on small- and medium-sized molecules. Future investigations could extend this study to larger systems. Indeed, the quality of EOM-CCSD deteriorates with increasing system size and becomes less accurate than EOM-CC2 for large systems.²¹⁹ It remains to be seen whether this observation holds true within the state-specific formalism.

■ ASSOCIATED CONTENT

Supporting Information

The Supporting Information is available free of charge at <https://pubs.acs.org/doi/10.1021/acs.jctc.4c00034>.


TD-CC data (XLS)

Geometries of borole and oxalyl fluoride, further statistical measures, TD-CCSD equations, raw data associated with each figure and table, and energies at different levels of theory in the considered basis sets (PDF)

■ AUTHOR INFORMATION

Corresponding Authors

Yann Damour – *Laboratoire de Chimie et Physique Quantiques (UMR 5626), Université de Toulouse, CNRS, UPS, 31000 Toulouse, France*; Email: yann.damour@irsamc.ups-tlse.fr

Fábris Kossoski – *Laboratoire de Chimie et Physique Quantiques (UMR 5626), Université de Toulouse, CNRS, UPS, 31000 Toulouse, France*;  orcid.org/0000-0002-1627-7093; Email: fabris.kossoski@irsamc.ups-tlse.fr

Pierre-François Loos – Laboratoire de Chimie et Physique Quantiques (UMR 5626), Université de Toulouse, CNRS, UPS, 31000 Toulouse, France; orcid.org/0000-0003-0598-7425; Email: loos@irsamc.ups-tlse.fr

Authors

Anthony Scemama – Laboratoire de Chimie et Physique Quantiques (UMR 5626), Université de Toulouse, CNRS, UPS, 31000 Toulouse, France; orcid.org/0000-0003-4955-7136

Denis Jacquemin – Nantes Université, CNRS, CEISAM UMR 6230, F-44000 Nantes, France; Institut Universitaire de France (IUF), F-75005 Paris, France; orcid.org/0000-0002-4217-0708

Complete contact information is available at:
<https://pubs.acs.org/10.1021/acs.jctc.4c00034>

Notes

The authors declare no competing financial interest.

ACKNOWLEDGMENTS

The authors thank Ajith Perera, Moneesha Ravi, Péter Szalay, and Rodney Bartlett for helpful discussions. This project has received funding from the European Research Council (ERC) under the European Union's Horizon 2020 research and innovation programme (grant agreement no. 863481). This work used the HPC resources from CALMIP (Toulouse) under allocation 2024-18005 and from the CCIPL/GliCID mesocenter installed in Nantes.

REFERENCES

- (1) Roos, B. O.; Andersson, K.; Fulscher, M. P.; Malmqvist, P.-A.; Serrano-Andrés, L. *Multiconfigurational Perturbation Theory: Applications in Electronic Spectroscopy*; Prigogine, I., Rice, S. A., Eds.; *Advances in Chemical Physics*; Wiley, New York, 1996; Vol. XCIII; pp 219–331.
- (2) Piecuch, P.; Kowalski, K.; Pimienta, I. S. O.; Mcguire, M. J. Recent advances in electronic structure theory: Method of moments of coupled-cluster equations and renormalized coupled-cluster approaches. *Int. Rev. Phys. Chem.* **2002**, *21*, 527–655.
- (3) Dreuw, A.; Head-Gordon, M. Single-Reference Ab Initio Methods for the Calculation of Excited States of Large Molecules. *Chem. Rev.* **2005**, *105*, 4009–4037.
- (4) Krylov, A. I. Spin-Flip Equation-of-Motion Coupled-Cluster Electronic Structure Method for a Description of Excited States, Bond Breaking, Diradicals, and Triradicals. *Acc. Chem. Res.* **2006**, *39*, 83–91.
- (5) Sneskov, K.; Christiansen, O. Excited State Coupled Cluster Methods. *Wiley Interdiscip. Rev.: Comput. Mol. Sci.* **2012**, *2*, 566–584.
- (6) González, L.; Escudero, D.; Serrano-Andrés, L. Progress and Challenges in the Calculation of Electronic Excited States. *ChemPhysChem* **2012**, *13*, 28–51.
- (7) Laurent, A. D.; Jacquemin, D. TD-DFT benchmarks: A review. *Int. J. Quantum Chem.* **2013**, *113*, 2019–2039.
- (8) Adamo, C.; Jacquemin, D. The Calculations of Excited-State Properties with Time-Dependent Density Functional Theory. *Chem. Soc. Rev.* **2013**, *42*, 845–856.
- (9) Ghosh, S.; Verma, P.; Cramer, C. J.; Gagliardi, L.; Truhlar, D. G. Combining Wave Function Methods with Density Functional Theory for Excited States. *Chem. Rev.* **2018**, *118*, 7249–7292.
- (10) Blase, X.; Duchemin, I.; Jacquemin, D.; Loos, P.-F. The Bethe–Salpeter Equation Formalism: From Physics to Chemistry. *J. Phys. Chem. Lett.* **2020**, *11*, 7371–7382.
- (11) Loos, P.-F.; Scemama, A.; Jacquemin, D. The Quest for Highly Accurate Excitation Energies: A Computational Perspective. *J. Phys. Chem. Lett.* **2020**, *11*, 2374–2383.
- (12) Hohenberg, P.; Kohn, W. Inhomogeneous Electron Gas. *Phys. Rev.* **1964**, *136*, B864–B871.
- (13) Kohn, W.; Sham, L. J. Self-Consistent Equations Including Exchange and Correlation Effects. *Phys. Rev.* **1965**, *140*, A1133–A1138.
- (14) Parr, R. G.; Weitao, Y. *Density-Functional Theory of Atoms and Molecules*; Oxford University Press: Oxford, England, UK, 1989.
- (15) Teale, A. M.; Helgaker, T.; Savin, A.; Adamo, C.; Aradi, B.; Arbuznikov, A. V.; Ayers, P. W.; Baerends, E. J.; Barone, V.; Calaminici, P.; et al. DFT exchange: sharing perspectives on the workhorse of quantum chemistry and materials science. *Phys. Chem. Chem. Phys.* **2022**, *24*, 28700–28781.
- (16) Runge, E.; Gross, E. K. U. Density-Functional Theory for Time-Dependent Systems. *Phys. Rev. Lett.* **1984**, *52*, 997–1000.
- (17) Burke, K.; Werschnik, J.; Gross, E. K. U. Time-dependent density functional theory: past, present, and future. *J. Chem. Phys.* **2005**, *123*, 062206.
- (18) Casida, M. E.; Huix-Rotllant, M. Progress in Time-Dependent Density-Functional Theory. *Annu. Rev. Phys. Chem.* **2012**, *63*, 287–323.
- (19) Huix-Rotllant, M.; Ferré, N.; Barbatti, M. *Quantum Chemistry and Dynamics of Excited States*; John Wiley & Sons Ltd.: Chichester, England, UK, 2020; pp 13–46.
- (20) Čížek, J. On the Correlation Problem in Atomic and Molecular Systems. Calculation of Wavefunction Components in Ursell-Type Expansion Using Quantum-Field Theoretical Methods. *J. Chem. Phys.* **1966**, *45*, 4256–4266.
- (21) Čížek, J. *Advances in Chemical Physics*; John Wiley & Sons, Ltd: Chichester, England, UK, 1969; pp 35–89.
- (22) Paldus, J. *Methods in Computational Molecular Physics*; Springer: Boston, MA; Boston, MA, USA, 1992; pp 99–194.
- (23) Crawford, T. D.; Schaefer, H. F. *Reviews in Computational Chemistry*; John Wiley & Sons, Ltd: Chichester, England, UK, 2000; pp 33–136.
- (24) Bartlett, R. J.; Musiał, M. Coupled-cluster theory in quantum chemistry. *Rev. Mod. Phys.* **2007**, *79*, 291–352.
- (25) Shavitt, I.; Bartlett, R. J. *Many-body Methods in Chemistry and Physics: MBPT and Coupled-Cluster Theory*; Cambridge University Press: Cambridge, England, UK, 2009.
- (26) Rowe, D. J. Equations-of-Motion Method and the Extended Shell Model. *Rev. Mod. Phys.* **1968**, *40*, 153–166.
- (27) Emrich, K. An extension of the coupled cluster formalism to excited states (I). *Nucl. Phys. A* **1981**, *351*, 379–396.
- (28) Sekino, H.; Bartlett, R. J. A linear response, coupled-cluster theory for excitation energy. *Int. J. Quantum Chem.* **1984**, *26*, 255–265.
- (29) Geertsen, J.; Rittby, M.; Bartlett, R. J. The equation-of-motion coupled-cluster method: Excitation energies of Be and CO. *Chem. Phys. Lett.* **1989**, *164*, 57–62.
- (30) Stanton, J. F.; Bartlett, R. J. The equation of motion coupled-cluster method. A systematic biorthogonal approach to molecular excitation energies, transition probabilities, and excited state properties. *J. Chem. Phys.* **1993**, *98*, 7029–7039.
- (31) Comeau, D. C.; Bartlett, R. J. The equation-of-motion coupled-cluster method. Applications to open- and closed-shell reference states. *Chem. Phys. Lett.* **1993**, *207*, 414–423.
- (32) Watts, J. D.; Bartlett, R. J. The inclusion of connected triple excitations in the equation-of-motion coupled-cluster method. *J. Chem. Phys.* **1994**, *101*, 3073–3078.
- (33) Monkhorst, H. J. Calculation of properties with the coupled-cluster method. *Int. J. Quantum Chem.* **1977**, *12*, 421–432.
- (34) Dalggaard, E.; Monkhorst, H. J. Some aspects of the time-dependent coupled-cluster approach to dynamic response functions. *Phys. Rev. A* **1983**, *28*, 1217–1222.
- (35) Koch, H.; Jørgensen, P. Coupled cluster response functions. *J. Chem. Phys.* **1990**, *93*, 3333–3344.
- (36) Koch, H.; Jensen, H. J. A.; Jørgensen, P.; Helgaker, T. Excitation Energies from the Coupled Cluster Singles and Doubles Linear Response Function (CCSDLR). Applications to Be, CH⁺, CO, and H₂ O. *J. Chem. Phys.* **1990**, *93*, 3345–3350.

- (37) Watson, M. A.; Chan, G. K.-L. Excited States of Butadiene to Chemical Accuracy: Reconciling Theory and Experiment. *J. Chem. Theory Comput.* **2012**, *8*, 4013–4018.
- (38) Shu, Y.; Truhlar, D. G. Doubly Excited Character or Static Correlation of the Reference State in the Controversial 2^1A_g State of *Trans*-Butadiene? *J. Am. Chem. Soc.* **2017**, *139*, 13770–13778.
- (39) Barca, G. M. J.; Gilbert, A. T. B.; Gill, P. M. W. Excitation Number: Characterizing Multiply Excited States. *J. Chem. Theory Comput.* **2018**, *14*, 9–13.
- (40) Loos, P.-F.; Boggio-Pasqua, M.; Scemama, A.; Caffarel, M.; Jacquemin, D. Reference Energies for Double Excitations. *J. Chem. Theory Comput.* **2019**, *15*, 1939–1956.
- (41) Ravi, M.; Park, Y. c.; Perera, A.; Bartlett, R. J. The intermediate state approach for doubly excited dark states in EOM-coupled-cluster theory. *J. Chem. Phys.* **2022**, *156*, 201102.
- (42) do Casal, M. T.; Toldo, J. M.; Barbatti, M.; Plasser, F. Classification of doubly excited molecular electronic states. *Chem. Sci.* **2023**, *14*, 4012–4026.
- (43) Szabo, A.; Ostlund, N. S. *Modern Quantum Chemistry*; McGraw-Hill: New York, 1989.
- (44) Werner, H.-J.; Meyer, W. A quadratically convergent MCSCF method for the simultaneous optimization of several states. *J. Chem. Phys.* **1981**, *74*, 5794–5801.
- (45) Diffenderfer, R. N.; Yarkony, D. R. Use of the state-averaged MCSCF procedure: application to radiative transitions in magnesium oxide. *J. Phys. Chem.* **1982**, *86*, 5098–5105.
- (46) Docken, K. K.; Hinze, J. LiH Potential Curves and Wavefunctions for $X^1\Sigma^+$, $A^1\Sigma^+$, $B^1\Pi$, $3\Sigma^+$, and 3Π . *J. Chem. Phys.* **1972**, *57*, 4928–4936.
- (47) Golab, J. T.; Yeager, D. L.; Jørgensen, P. Proper characterization of MC SCF stationary points. *Chem. Phys.* **1983**, *78*, 175–199.
- (48) Ziegler, T.; Rauk, A.; Baerends, E. J. On the calculation of multiplet energies by the hartree-fock-slater method. *Theor. Chim. Acta* **1977**, *43*, 261–271.
- (49) Gilbert, A. T. B.; Besley, N. A.; Gill, P. M. W. Self-Consistent Field Calculations of Excited States Using the Maximum Overlap Method (MOM). *J. Phys. Chem. A* **2008**, *112*, 13164–13171.
- (50) Kowalczyk, T.; Yost, S. R.; Voorhis, T. V. Assessment of the Δ SCF density functional theory approach for electronic excitations in organic dyes. *J. Chem. Phys.* **2011**, *134*, 054128.
- (51) Filatov, M.; Shaik, S. A spin-restricted ensemble-referenced Kohn–Sham method and its application to diradicaloid situations. *Chem. Phys. Lett.* **1999**, *304*, 429–437.
- (52) Kowalczyk, T.; Tsuchimochi, T.; Chen, P.-T.; Top, L.; Van Voorhis, T. Excitation energies and Stokes shifts from a restricted open-shell Kohn–Sham approach. *J. Chem. Phys.* **2013**, *138*, 164101.
- (53) Levi, G.; Ivanov, A. V.; Jónsson, H. Variational Density Functional Calculations of Excited States via Direct Optimization. *J. Chem. Theory Comput.* **2020**, *16*, 6968–6982.
- (54) Levi, G.; Ivanov, A. V.; Jónsson, H. Variational calculations of excited states via direct optimization of the orbitals in DFT. *Faraday Discuss.* **2020**, *224*, 448–466.
- (55) Hait, D.; Head-Gordon, M. Excited State Orbital Optimization via Minimizing the Square of the Gradient: General Approach and Application to Singly and Doubly Excited States via Density Functional Theory. *J. Chem. Theory Comput.* **2020**, *16*, 1699–1710.
- (56) Hait, D.; Head-Gordon, M. Orbital Optimized Density Functional Theory for Electronic Excited States. *J. Phys. Chem. Lett.* **2021**, *12*, 4517–4529.
- (57) Cunha, L. A.; Hait, D.; Kang, R.; Mao, Y.; Head-Gordon, M. Relativistic Orbital-Optimized Density Functional Theory for Accurate Core-Level Spectroscopy. *J. Phys. Chem. Lett.* **2022**, *13*, 3438–3449.
- (58) Toffoli, D.; Quarin, M.; Fronzoni, G.; Stener, M. Accurate Vertical Excitation Energies of BODIPY/Aza-BODIPY Derivatives from Excited-State Mean-Field Calculations. *J. Phys. Chem. A* **2022**, *126*, 7137–7146.
- (59) Shea, J. A. R.; Neuscamman, E. Communication: A mean field platform for excited state quantum chemistry. *J. Chem. Phys.* **2018**, *149*, 081101.
- (60) Barca, G.; Gilbert, A. T. B.; Gill, P. M. W. Simple Models for Difficult Electronic Excitations. *J. Chem. Theory Comput.* **2018**, *14*, 1501–1509.
- (61) Shea, J. A. R.; Gwin, E.; Neuscamman, E. A Generalized Variational Principle with Applications to Excited State Mean Field Theory. *J. Chem. Theory Comput.* **2020**, *16*, 1526–1540.
- (62) Hardikar, T. S.; Neuscamman, E. A self-consistent field formulation of excited state mean field theory. *J. Chem. Phys.* **2020**, *153*, 164108.
- (63) Carter-Fenk, K.; Herbert, J. M. State-Targeted Energy Projection: A Simple and Robust Approach to Orbital Relaxation of Non-Aufbau Self-Consistent Field Solutions. *J. Chem. Theory Comput.* **2020**, *16*, 5067–5082.
- (64) Wibowo, M.; Huynh, B. C.; Cheng, C. Y.; Irons, T. J. P.; Teale, A. M. Understanding ground and excited-state molecular structure in strong magnetic fields using the maximum overlap method. *Mol. Phys.* **2023**, *121*, No. e2152748.
- (65) Schmerwitz, Y. L. A.; Ivanov, A. V.; Jonsson, E. O.; Jonsson, H.; Levi, G. Variational Density Functional Calculations of Excited States: Conical Intersection and Avoided Crossing in Ethylene Bond Twisting. *J. Phys. Chem. Lett.* **2022**, *13*, 3990–3999.
- (66) Schmerwitz, Y. L. A.; Levi, G.; Jónsson, H. Calculations of Excited Electronic States by Converging on Saddle Points Using Generalized Mode Following. *J. Chem. Theory Comput.* **2023**, *19*, 3634–3651.
- (67) Das, G.; Wahl, A. C. Extended Hartree–Fock Wavefunctions: Optimized Valence Configurations for H₂ and Li₂, Optimized Double Configurations for F₂. *J. Chem. Phys.* **1966**, *44*, 87–96.
- (68) Das, G. Multiconfiguration self-consistent field (MCSCF) theory for excited states. *J. Chem. Phys.* **1973**, *58*, 5104–5110.
- (69) Roos, B. O.; Taylor, P. R.; Sigbahn, P. E. M. A complete active space SCF method (CASSCF) using a density matrix formulated super-CI approach. *Chem. Phys.* **1980**, *48*, 157–173.
- (70) Roos, B. O. The complete active space SCF method in a fock-matrix-based super-CI formulation. *Int. J. Quantum Chem.* **1980**, *18*, 175–189.
- (71) Malmqvist, P. A.; Rendell, A.; Roos, B. O. The restricted active space self-consistent-field method, implemented with a split graph unitary group approach. *J. Phys. Chem.* **1990**, *94*, 5477–5482.
- (72) Roos, B. O.; Lindh, R.; Malmqvist, P. Å.; Veryazov, V.; Widmark, P.-O. *Multiconfigurational Quantum Chemistry*; Wiley: Hoboken, NJ, USA, 2016.
- (73) Andersson, K.; Malmqvist, P. A.; Roos, B. O.; Sadlej, A. J.; Wolinski, K. Second-order perturbation theory with a CASSCF reference function. *J. Phys. Chem.* **1990**, *94*, 5483–5488.
- (74) Andersson, K.; Malmqvist, P.-Å.; Roos, B. O. Second-order perturbation theory with a complete active space self-consistent field reference function. *J. Chem. Phys.* **1992**, *96*, 1218–1226.
- (75) Finley, J.; Malmqvist, P.-Å.; Roos, B. O.; Serrano-Andrés, L. The multi-state CASPT2 method. *Chem. Phys. Lett.* **1998**, *288*, 299–306.
- (76) Angeli, C.; Cimiraglia, R.; Evangelisti, S.; Leininger, T.; Malrieu, J.-P. Introduction of *n*-electron valence states for multi-reference perturbation theory. *J. Chem. Phys.* **2001**, *114*, 10252–10264.
- (77) Angeli, C.; Cimiraglia, R.; Malrieu, J.-P. *n*-electron valence state perturbation theory: A spinless formulation and an efficient implementation of the strongly contracted and of the partially contracted variants. *J. Chem. Phys.* **2002**, *117*, 9138–9153.
- (78) Battaglia, S.; Fdez; Galván, I.; Lindh, R. *Theoretical and Computational Photochemistry*; Elsevier: Waltham, MA, USA, 2023; pp 135–162.
- (79) Tran, L. N.; Shea, J. A. R.; Neuscamman, E. Tracking Excited States in Wave Function Optimization Using Density Matrices and Variational Principles. *J. Chem. Theory Comput.* **2019**, *15*, 4790–4803.

- (80) Tran, L. N.; Neuscamman, E. Improving Excited-State Potential Energy Surfaces via Optimal Orbital Shapes. *J. Phys. Chem. A* **2020**, *124*, 8273–8279.
- (81) Burton, H. G. A.; Wales, D. J. Energy Landscapes for Electronic Structure. *J. Chem. Theory Comput.* **2021**, *17*, 151–169.
- (82) Burton, H. G. Energy Landscape of State-Specific Electronic Structure Theory. *J. Chem. Theory Comput.* **2022**, *18*, 1512–1526.
- (83) Marie, A.; Burton, H. G. A. Excited States, Symmetry Breaking, and Unphysical Solutions in State-Specific CASSCF Theory. *J. Phys. Chem. A* **2023**, *127*, 4538–4552.
- (84) Kossoski, F.; Loos, P.-F. State-Specific Configuration Interaction for Excited States. *J. Chem. Theory Comput.* **2023**, *19*, 2258–2269.
- (85) Bender, C. F.; Davidson, E. R. Studies in Configuration Interaction: The First-Row Diatomic Hydrides. *Phys. Rev.* **1969**, *183*, 23–30.
- (86) Huron, B.; Malrieu, J. P.; Rancurel, P. Iterative perturbation calculations of ground and excited state energies from multiconfigurational zeroth-order wavefunctions. *J. Chem. Phys.* **1973**, *58*, 5745–5759.
- (87) Buenker, R. J.; Peyerimhoff, S. D. Individualized configuration selection in CI calculations with subsequent energy extrapolation. *Theor. Chim. Acta* **1974**, *35*, 33–58.
- (88) Evangelisti, S.; Daudey, J.-P.; Malrieu, J.-P. Convergence of an improved CIPSI algorithm. *Chem. Phys.* **1983**, *75*, 91–102.
- (89) Angeli, C.; Cimiraglia, R. Multireference perturbation CI IV. Selection procedure for one-electron properties. *Theor. Chem. Acc.* **2001**, *105*, 259–264.
- (90) Liu, W.; Hoffmann, M. R. iCI: Iterative CI toward full CI. *J. Chem. Theory Comput.* **2016**, *12*, 1169–1178.
- (91) Harrison, R. J. Approximating full configuration interaction with selected configuration interaction and perturbation theory. *J. Chem. Phys.* **1991**, *94*, 5021–5031.
- (92) Giner, E.; Scemama, A.; Caffarel, M. Using perturbatively selected configuration interaction in quantum Monte Carlo calculations. *Can. J. Chem.* **2013**, *91*, 879–885.
- (93) Giner, E.; Scemama, A.; Caffarel, M. Fixed-node diffusion Monte Carlo potential energy curve of the fluorine molecule F₂ using selected configuration interaction trial wavefunctions. *J. Chem. Phys.* **2015**, *142*, 044115.
- (94) Holmes, A. A.; Tubman, N. M.; Umrigar, C. J. Heat-Bath Configuration Interaction: An Efficient Selected Configuration Interaction Algorithm Inspired by Heat-Bath Sampling. *J. Chem. Theory Comput.* **2016**, *12*, 3674–3680.
- (95) Schriber, J. B.; Evangelista, F. A. Communication: An adaptive configuration interaction approach for strongly correlated electrons with tunable accuracy. *J. Chem. Phys.* **2016**, *144*, 161106.
- (96) Tubman, N. M.; Lee, J.; Takeshita, T. Y.; Head-Gordon, M.; Whaley, K. B. A deterministic alternative to the full configuration interaction quantum Monte Carlo method. *J. Chem. Phys.* **2016**, *145*, 044112.
- (97) Sharma, S.; Holmes, A. A.; Jeanmairet, G.; Alavi, A.; Umrigar, C. J. Semistochastic Heat-Bath Configuration Interaction Method: Selected Configuration Interaction with Semistochastic Perturbation Theory. *J. Chem. Theory Comput.* **2017**, *13*, 1595–1604.
- (98) Coe, J. P. Machine Learning Configuration Interaction. *J. Chem. Theory Comput.* **2018**, *14*, 5739–5749.
- (99) Garniron, Y.; Applencourt, T.; Gasperich, K.; Benali, A.; Ferté, A.; Paquier, J.; Pradines, B.; Assaraf, R.; Reinhardt, P.; Toulouse, J.; et al. Quantum Package 2.0: An Open-Source Determinant-Driven Suite of Programs. *J. Chem. Theory Comput.* **2019**, *15*, 3591–3609.
- (100) Zhang, N.; Liu, W.; Hoffmann, M. R. Iterative Configuration Interaction with Selection. *J. Chem. Theory Comput.* **2020**, *16*, 2296–2316.
- (101) Zhang, N.; Liu, W.; Hoffmann, M. R. Further Development of iCIPT2 for Strongly Correlated Electrons. *J. Chem. Theory Comput.* **2021**, *17*, 949–964.
- (102) Mussard, B.; Sharma, S. One-Step Treatment of Spin–Orbit Coupling and Electron Correlation in Large Active Spaces. *J. Chem. Theory Comput.* **2018**, *14*, 154–165.
- (103) Chien, A. D.; Holmes, A. A.; Otten, M.; Umrigar, C. J.; Sharma, S.; Zimmerman, P. M. Excited States of Methylene, Polyenes, and Ozone from Heat-Bath Configuration Interaction. *J. Phys. Chem. A* **2018**, *122*, 2714–2722.
- (104) Loos, P.-F.; Damour, Y.; Scemama, A. The performance of CIPSI on the ground state electronic energy of benzene. *J. Chem. Phys.* **2020**, *153*, 176101.
- (105) Yao, Y.; Giner, E.; Li, J.; Toulouse, J.; Umrigar, C. J. Almost exact energies for the Gaussian-2 set with the semistochastic heat-bath configuration interaction method. *J. Chem. Phys.* **2020**, *153*, 124117.
- (106) Damour, Y.; Vêril, M.; Kossoski, F.; Caffarel, M.; Jacquemin, D.; Scemama, A.; Loos, P.-F. Accurate full configuration interaction correlation energy estimates for five- and six-membered rings. *J. Chem. Phys.* **2021**, *155*, 134104.
- (107) Yao, Y.; Umrigar, C. J. Orbital Optimization in Selected Configuration Interaction Methods. *J. Chem. Theory Comput.* **2021**, *17*, 4183–4194.
- (108) Larsson, H. R.; Zhai, H.; Umrigar, C. J.; Chan, G. K.-L. The Chromium Dimer: Closing a Chapter of Quantum Chemistry. *J. Am. Chem. Soc.* **2022**, *144*, 15932–15937.
- (109) Coe, J. P.; Moreno Carrascosa, A.; Simmermacher, M.; Kirrander, A.; Paterson, M. J. Efficient Computation of Two-Electron Reduced Density Matrices via Selected Configuration Interaction. *J. Chem. Theory Comput.* **2022**, *18*, 6690–6699.
- (110) Holmes, A. A.; Umrigar, C. J.; Sharma, S. Excited states using semistochastic heat-bath configuration interaction. *J. Chem. Phys.* **2017**, *147*, 164111.
- (111) Eriksen, J. J.; Anderson, T. A.; Deustua, J. E.; Ghanem, K.; Hait, D.; Hoffmann, M. R.; Lee, S.; Levine, D. S.; Magoulas, I.; Shen, J.; et al. The Ground State Electronic Energy of Benzene. *J. Phys. Chem. Lett.* **2020**, *11*, 8922–8929.
- (112) Damour, Y.; Quintero-Monsebaiz, R.; Caffarel, M.; Jacquemin, D.; Kossoski, F.; Scemama, A.; Loos, P.-F. Ground- and Excited-State Dipole Moments and Oscillator Strengths of Full Configuration Interaction Quality. *J. Chem. Theory Comput.* **2023**, *19*, 221–234.
- (113) Lee, J.; Small, D. W.; Head-Gordon, M. Excited states via coupled cluster theory without equation-of-motion methods: Seeking higher roots with application to doubly excited states and double core hole states. *J. Chem. Phys.* **2019**, *151*, 214103.
- (114) Mayhall, N. J.; Raghavachari, K. Multiple Solutions to the Single-Reference CCSD Equations for NiH. *J. Chem. Theory Comput.* **2010**, *6*, 2714–2720.
- (115) Dreuw, A.; Hoffmann, M. The inverted singlet–triplet gap: a vanishing myth? *Front. Chem.* **2023**, *11*, 1239604.
- (116) Rishi, V.; Ravi, M.; Perera, A.; Bartlett, R. J. Dark Doubly Excited States with Modified Coupled Cluster Models: A Reliable Compromise between Cost and Accuracy? *J. Phys. Chem. A* **2023**, *127*, 828–834.
- (117) Zheng, X.; Cheng, L. Performance of Delta-Coupled-Cluster Methods for Calculations of Core-Ionization Energies of First-Row Elements. *J. Chem. Theory Comput.* **2019**, *15*, 4945–4955.
- (118) Zheng, X.; Liu, J.; Doumy, G.; Young, L.; Cheng, L. Heterosite Double Core Ionization Energies with Sub-electronvolt Accuracy from Delta-Coupled-Cluster Calculations. *J. Phys. Chem. A* **2020**, *124*, 4413–4426.
- (119) Tsuru, S.; Vidal, M. L.; Pápai, M.; Krylov, A. I.; Möller, K. B.; Coriani, S. An assessment of different electronic structure approaches for modeling time-resolved x-ray absorption spectroscopy. *Struct. Dyn.* **2021**, *8*, 024101.
- (120) Matz, F.; Jagau, T.-C. Molecular Auger decay rates from complex-variable coupled-cluster theory. *J. Chem. Phys.* **2022**, *156*, 114117.
- (121) Jayadev, N. K.; Ferino-Pérez, A.; Matz, F.; Krylov, A. I.; Jagau, T.-C. The Auger spectrum of benzene. *J. Chem. Phys.* **2023**, *158*, 064109.

- (122) Matz, F.; Jagau, T.-C. Channel-specific core-valence projectors for determining partial Auger decay widths. *Mol. Phys.* **2023**, *121*, No. e2105270.
- (123) Arias-Martinez, J. E.; Cunha, L. A.; Oosterbaan, K. J.; Lee, J.; Head-Gordon, M. Accurate core excitation and ionization energies from a state-specific coupled-cluster singles and doubles approach. *Phys. Chem. Chem. Phys.* **2022**, *24*, 20728–20741.
- (124) Kats, D.; Manby, F. R. Communication: The distinguishable cluster approximation. *J. Chem. Phys.* **2013**, *139*, 021102.
- (125) Kats, D. Communication: The distinguishable cluster approximation. II. The role of orbital relaxation. *J. Chem. Phys.* **2014**, *141*, 061101.
- (126) Schraivogel, T.; Kats, D. Accuracy of the distinguishable cluster approximation for triple excitations for open-shell molecules and excited states. *J. Chem. Phys.* **2021**, *155*, 064101.
- (127) Kossoski, F.; Marie, A.; Scemama, A.; Caffarel, M.; Loos, P.-F. Excited States from State-Specific Orbital-Optimized Pair Coupled Cluster. *J. Chem. Theory Comput.* **2021**, *17*, 4756–4768.
- (128) Marie, A.; Kossoski, F.; Loos, P.-F. Variational coupled cluster for ground and excited states. *J. Chem. Phys.* **2021**, *155*, 104105.
- (129) Živković, T. P. Existence and Reality of Solutions of the Coupled-Cluster Equations. *Int. J. Quantum Chem.* **1977**, *12*, 413–420.
- (130) Živković, T. P.; Monkhorst, H. J. Analytic Connection between Configuration–Interaction and Coupled-cluster Solutions. *J. Math. Phys.* **1978**, *19*, 1007–1022.
- (131) Adamowicz, L.; Bartlett, R. J. Direct Coupled Cluster Calculations on Excited States. *Int. J. Quantum Chem.* **1985**, *28*, 217–220.
- (132) Jankowski, J.; Kowalski, K.; Jankowski, P. Applicability of Single-Reference Coupled-Cluster Methods to Excited States. A Model Study. *Chem. Phys. Lett.* **1994**, *222*, 608–614.
- (133) Jankowski, K.; Kowalski, K.; Jankowski, P. Multiple Solutions of the Single-Reference Coupled-Cluster Equations. I. H4Model Revisited. *Int. J. Quantum Chem.* **1994**, *50*, 353–367.
- (134) Jankowski, K.; Kowalski, K.; Jankowski, P. Multiple Solutions of the Single-Reference Coupled-Cluster Equations. II. Alternative Reference States. *Int. J. Quantum Chem.* **1995**, *53*, 501–514.
- (135) Verschelde, J.; Cools, R. Symmetric Homotopy Construction. *J. Comput. Appl. Math.* **1994**, *50*, 575–592.
- (136) Kowalski, K.; Jankowski, K. Full Solution to the Coupled-Cluster Equations: The H4 Model. *Chem. Phys. Lett.* **1998**, *290*, 180–188.
- (137) Kowalski, K.; Jankowski, K. Towards Complete Solutions to Systems of Nonlinear Equations of Many-Electron Theories. *Phys. Rev. Lett.* **1998**, *81*, 1195–1198.
- (138) Jankowski, K.; Kowalski, K. Physical and Mathematical Content of Coupled-Cluster Equations. II. On the Origin of Irregular Solutions and Their Elimination via Symmetry Adaptation. *J. Chem. Phys.* **1999**, *110*, 9345–9352.
- (139) Jankowski, K.; Kowalski, K. Physical and Mathematical Content of Coupled-Cluster Equations. III. Model Studies of Dissociation Processes for Various Reference States. *J. Chem. Phys.* **1999**, *111*, 2940–2951.
- (140) Jankowski, K.; Kowalski, K. Physical and Mathematical Content of Coupled-Cluster Equations. IV. Impact of Approximations to the Cluster Operator on the Structure of Solutions. *J. Chem. Phys.* **1999**, *111*, 2952–2959.
- (141) Jankowski, K.; Kowalski, K. Physical and Mathematical Content of Coupled-Cluster Equations: Correspondence between Coupled-Cluster and Configuration–Interaction Solutions. *J. Chem. Phys.* **1999**, *110*, 3714–3729.
- (142) Kowalski, K.; Piecuch, P. Complete Set of Solutions of Multireference Coupled-Cluster Equations: The State-Universal Formalism. *Phys. Rev. A* **2000**, *61*, 052506.
- (143) Kowalski, K.; Piecuch, P. Complete set of solutions of the generalized Bloch equation. *Int. J. Quantum Chem.* **2000**, *80*, 757–781.
- (144) Piecuch, P.; Kowalski, K. *Computational Chemistry: Reviews of Current Trends*; World Scientific, 2000; Vol. 5, pp 1–104.
- (145) Csirik, M. A.; Laestadius, A. Coupled-Cluster theory revisited: Part I: Discretization. *ESAIM: Math. Modell. Numer. Anal.* **2023**, *57*, 645–670.
- (146) Csirik, M. A.; Laestadius, A. Coupled-Cluster theory revisited: Part II: Analysis of the single-reference Coupled-Cluster equations. *ESAIM: Math. Modell. Numer. Anal.* **2023**, *57*, 545–583.
- (147) Faulstich, F. M.; Oster, M. Coupled Cluster Theory: Toward an Algebraic Geometry Formulation. *J. Appl. Algebra Geom.* **2024**, *8*, 138–188.
- (148) Faulstich, F. M.; Laestadius, A. Homotopy continuation methods for coupled-cluster theory in quantum chemistry. *Mol. Phys.* **2023**, *0*, No. e2258599.
- (149) Szalay, P. G.; Müller, T.; Gidofalvi, G.; Lischka, H.; Shepard, R. Multiconfiguration self-consistent field and multireference configuration interaction methods and applications. *Chem. Rev.* **2012**, *112*, 108–181.
- (150) Lischka, H.; Nachtigallová, D.; Aquino, A. J. A.; Szalay, P. G.; Plasser, F.; Machado, F. B. C.; Barbatti, M. Multireference Approaches for Excited States of Molecules. *Chem. Rev.* **2018**, *118*, 7293–7361.
- (151) Tuckman, H.; Neuscamman, E. Excited-State-Specific Pseudoprojected Coupled-Cluster Theory. *J. Chem. Theory Comput.* **2023**, *19*, 6160–6171.
- (152) Tuckman, H.; Neuscamman, E. Aufbau Suppressed Coupled Cluster Theory for Electronically Excited States. *arXiv* **2023**, arXiv:2311.13576.
- (153) Musial, M.; Bartlett, R. J. Multireference Fock-space coupled-cluster and equation-of-motion coupled-cluster theories: The detailed interconnections. *J. Chem. Phys.* **2008**, *129*, 134105.
- (154) Lyakh, D. I.; Musial, M.; Lotrich, V. F.; Bartlett, R. J. Multireference Nature of Chemistry: The Coupled-Cluster View. *Chem. Rev.* **2012**, *112*, 182–243.
- (155) Köhn, A.; Hanauer, M.; Mück, L. A.; Jagau, T.-C.; Gauss, J. State-specific multireference coupled-cluster theory. *Wiley Interdiscip. Rev.: Comput. Mol. Sci.* **2013**, *3*, 176–197.
- (156) Evangelista, F. A. Perspective: Multireference coupled cluster theories of dynamical electron correlation. *J. Chem. Phys.* **2018**, *149*, 030901.
- (157) Lindgren, I. A coupled-cluster approach to the many-body perturbation theory for open-shell systems. *Int. J. Quantum Chem.* **1978**, *14*, 33–58.
- (158) Haque, M. A.; Mukherjee, D. Application of cluster expansion techniques to open shells: Calculation of difference energies. *J. Chem. Phys.* **1984**, *80*, 5058–5069.
- (159) Sinha, D.; Mukhopadhyay, S. Kr.; Prasad, M. D.; Mukherjee, D. Molecular applications of open-shell coupled cluster theory for energy difference calculations: ionization and auger spectra of F₂. *Chem. Phys. Lett.* **1986**, *125*, 213–217.
- (160) Pal, S.; Rittby, M.; Bartlett, R. J.; Sinha, D.; Mukherjee, D. Multireference coupled-cluster methods using an incomplete model space: Application to ionization potentials and excitation energies of formaldehyde. *Chem. Phys. Lett.* **1987**, *137*, 273–278.
- (161) Pal, S.; Rittby, M.; Bartlett, R. J.; Sinha, D.; Mukherjee, D. Molecular applications of multireference coupled-cluster methods using an incomplete model space: Direct calculation of excitation energies. *J. Chem. Phys.* **1988**, *88*, 4357–4366.
- (162) Jeziorski, B.; Paldus, J. Valence universal exponential ansatz and the cluster structure of multireference configuration interaction wave function. *J. Chem. Phys.* **1989**, *90*, 2714–2731.
- (163) Chaudhuri, R.; Mukhopadhyay, D.; Mukherjee, D. Applications of open-shell coupled cluster theory using an eigenvalue-independent partitioning technique: Approximate inclusion of triples in IP calculations. *Chem. Phys. Lett.* **1989**, *162*, 393–398.
- (164) Landau, A.; Eliav, E.; Kaldor, U. Intermediate Hamiltonian Fock-space coupled-cluster method. *Chem. Phys. Lett.* **1999**, *313*, 399–403.

- (165) Landau, A.; Eliav, E.; Ishikawa, Y.; Kaldor, U. Intermediate Hamiltonian Fock-space coupled-cluster method: Excitation energies of barium and radium. *J. Chem. Phys.* **2000**, *113*, 9905–9910.
- (166) Jeziorski, B.; Monkhorst, H. J. Coupled-cluster method for multideterminantal reference states. *Phys. Rev. A* **1981**, *24*, 1668–1681.
- (167) Lindgren, I.; Mukherjee, D. On the connectivity criteria in the open-shell coupled-cluster theory for general model spaces. *Phys. Rep.* **1987**, *151*, 93–127.
- (168) Mukherjee, D.; Pal, S. *Adv. Quantum Chem.*; Academic Press: Cambridge, MA, USA, 1989; Vol. 20, pp 291–373.
- (169) Kucharski, S. A.; Bartlett, R. J. Hilbert space multireference coupled-cluster methods. I. The single and double excitation model. *J. Chem. Phys.* **1991**, *95*, 8227–8238.
- (170) Balková, A.; Kucharski, S. A.; Meissner, L.; Bartlett, R. J. The multireference coupled-cluster method in Hilbert space: An incomplete model space application to the LiH molecule. *J. Chem. Phys.* **1991**, *95*, 4311–4316.
- (171) Balková, A.; Kucharski, S. A.; Meissner, L.; Bartlett, R. J. A Hilbert space multi-reference coupled-cluster study of the H4 model system. *Theor. Chim. Acta* **1991**, *80*, 335–348.
- (172) Balková, A.; Bartlett, R. J. Coupled-cluster method for open-shell singlet states. *Chem. Phys. Lett.* **1992**, *193*, 364–372.
- (173) Kucharski, S. A.; Balková, A.; Szalay, P. G.; Bartlett, R. J. Hilbert space multireference coupled-cluster methods. II. A model study on H8. *J. Chem. Phys.* **1992**, *97*, 4289–4300.
- (174) Paldus, J.; Piecuch, P.; Pylypow, L.; Jeziorski, B. Application of Hilbert-Space Coupled-Cluster Theory to Simple (H₂)₂ Model Systems: Planar Models. *Phys. Rev. A* **1993**, *47*, 2738–2782.
- (175) Mášik, J.; Hubač, I. *Adv. Quantum Chem.*; Academic Press: Cambridge, MA, USA, 1998; Vol. 31, pp 75–104.
- (176) Pittner, J.; Nachtigall, P.; Čársky, P.; Mášik, J.; Hubač, I. Assessment of the single-root multireference Brillouin–Wigner coupled-cluster method: Test calculations on CH₂, SiH₂, and twisted ethylene. *J. Chem. Phys.* **1999**, *110*, 10275–10282.
- (177) Hubač, I.; Pittner, J.; Čársky, P. Size-extensivity correction for the state-specific multireference Brillouin–Wigner coupled-cluster theory. *J. Chem. Phys.* **2000**, *112*, 8779–8784.
- (178) Pittner, J. Continuous transition between Brillouin–Wigner and Rayleigh–Schrödinger perturbation theory, generalized Bloch equation, and Hilbert space multireference coupled cluster. *J. Chem. Phys.* **2003**, *118*, 10876–10889.
- (179) Li, X.; Paldus, J. The general-model-space state-universal coupled-cluster method exemplified by the LiH molecule. *J. Chem. Phys.* **2003**, *119*, 5346–5357.
- (180) Li, X.; Paldus, J. Performance of the general-model-space state-universal coupled-cluster method. *J. Chem. Phys.* **2004**, *120*, 5890–5902.
- (181) Mahapatra, U. S.; Datta, B.; Bandyopadhyay, B.; Mukherjee, D. *Adv. Quantum Chem.*; Academic Press: Cambridge, MA, USA, 1998; Vol. 30, pp 163–193.
- (182) Das, S.; Mukherjee, D.; Kállay, M. Full implementation and benchmark studies of Mukherjee’s state-specific multireference coupled-cluster ansatz. *J. Chem. Phys.* **2010**, *132*, 074103.
- (183) Garniron, Y.; Giner, E.; Malrieu, J.-P.; Scemama, A. Alternative definition of excitation amplitudes in multi-reference state-specific coupled cluster. *J. Chem. Phys.* **2017**, *146*, 154107.
- (184) Malrieu, J. P.; Durand, P.; Daudey, J. P. Intermediate Hamiltonians as a new class of effective Hamiltonians. *J. Phys. A: Math. Gen.* **1985**, *18*, 809–826.
- (185) Meissner, L.; Nooijen, M. Effective and intermediate Hamiltonians obtained by similarity transformations. *J. Chem. Phys.* **1995**, *102*, 9604–9614.
- (186) Meissner, L. Fock-space coupled-cluster method in the intermediate Hamiltonian formulation: Model with singles and doubles. *J. Chem. Phys.* **1998**, *108*, 9227–9235.
- (187) Giner, E.; David, G.; Scemama, A.; Malrieu, J. P. A simple approach to the state-specific MR-CC using the intermediate Hamiltonian formalism. *J. Chem. Phys.* **2016**, *144*, 064101.
- (188) Giner, E.; Angeli, C.; Garniron, Y.; Scemama, A.; Malrieu, J.-P. A Jeziorski-Monkhorst fully uncontracted multi-reference perturbative treatment. I. Principles, second-order versions, and tests on ground state potential energy curves. *J. Chem. Phys.* **2017**, *146*, 224108.
- (189) Balková, A.; Bartlett, R. J. The two-determinant coupled-cluster method for electric properties of excited electronic states: The lowest 1B1 and 3B1 states of the water molecule. *J. Chem. Phys.* **1993**, *99*, 7907–7915.
- (190) Balková, A.; Bartlett, R. J. A multireference coupled-cluster study of the ground state and lowest excited states of cyclobutadiene. *J. Chem. Phys.* **1994**, *101*, 8972–8987.
- (191) Szalay, P. G.; Bartlett, R. J. Analytic energy gradients for the two-determinant coupled cluster method with application to singlet excited states of butadiene and ozone. *J. Chem. Phys.* **1994**, *101*, 4936–4944.
- (192) Lutz, J. J.; Nooijen, M.; Perera, A.; Bartlett, R. J. Reference dependence of the two-determinant coupled-cluster method for triplet and open-shell singlet states of biradical molecules. *J. Chem. Phys.* **2018**, *148*, 164102.
- (193) Piecuch, P.; Paldus, J. Orthogonally spin-adapted multi-reference Hilbert space coupled-cluster formalism: diagrammatic formulation. *Theor. Chim. Acta* **1992**, *83*, 69–103.
- (194) Piecuch, P.; Toboła, R.; Paldus, J. Approximate account of connected quadruply excited clusters in multi-reference Hilbert space coupled-cluster theory. Application to planar H4 models. *Chem. Phys. Lett.* **1993**, *210*, 243–252.
- (195) Piecuch, P.; Paldus, J. Application of Hilbert-space coupled-cluster theory to simple (H₂)₂ model systems. II. Nonplanar models. *Phys. Rev. A* **1994**, *49*, 3479–3514.
- (196) Li, X.; Piecuch, P.; Paldus, J. A study of 1A1–3B1 separation in CH₂ using orthogonally spin-adapted state-universal and state-specific coupled-cluster methods. *Chem. Phys. Lett.* **1994**, *224*, 267–274.
- (197) Piecuch, P.; Paldus, J. Orthogonally spin-adapted state-universal coupled-cluster formalism: Implementation of the complete two-reference theory including cubic and quartic coupling terms. *J. Chem. Phys.* **1994**, *101*, 5875–5890.
- (198) Piecuch, P.; Li, X.; Paldus, J. An ab initio determination of ¹A₁–³B₁ energy gap in CH₂ using orthogonally spin-adapted state-universal and state-specific coupled-cluster methods. *Chem. Phys. Lett.* **1994**, *230*, 377–386.
- (199) Piecuch, P.; Paldus, J. Property Evaluation Using the Two-Reference State-Universal Coupled-Cluster Method. *J. Phys. Chem.* **1995**, *99*, 15354–15368.
- (200) Sarkar, R.; Boggio-Pasqua, M.; Loos, P. F.; Jacquemin, D. Benchmarking TD-DFT and Wave Function Methods for Oscillator Strengths and Excited-State Dipole Moments. *J. Chem. Theory Comput.* **2021**, *17*, 1117–1132.
- (201) Chrayteh, A.; Blondel, A.; Loos, P.-F.; Jacquemin, D. Mountaineering Strategy to Excited States: Highly Accurate Oscillator Strengths and Dipole Moments of Small Molecules. *J. Chem. Theory Comput.* **2021**, *17*, 416–438.
- (202) Rubin, N. C.; DePrince, A. E. p†q: a tool for prototyping many-body methods for quantum chemistry. *Mol. Phys.* **2021**, *119*, No. e1954709.
- (203) Evangelista, F. A. Automatic derivation of many-body theories based on general Fermi vacua. *J. Chem. Phys.* **2022**, *157*, 064111.
- (204) SimpleWick – Software Heritage archive, 2023 <https://archive.softwareheritage.org/swh:1:dir:e93480d3a1d26d5827a44d3543600b08e2ed66cc;origin=https://github.com/LCPQ/SimpleWick;visit=swh:1:snp:61c77fef95b602640446d88150fe469cfb2d0dc7;anchor=swh:1:rev:b0ca4f2019885e747ecbd68cdef5fa0ecc7b58a2> (accessed Dec 28, 2023).
- (205) Wick, G. C. The Evaluation of the Collision Matrix. *Phys. Rev.* **1950**, *80*, 268–272.
- (206) Gen_Eq_TDCC – Software Heritage archive, 2023. <https://archive.softwareheritage.org/swh:1:dir:9975d3d9a23e175c3b33c0d81a891793ee6c09a7;origin=https://doi.org/10.1021/acs.jctc.4c00034>

https://github.com/LCPQ/Gen_Eq_TDCC;visit=swh:1:snp:1c49be972d0fb80b8647028ec07a030b2c4ef961;anchor=swh:1:rev:0b494efb16263192e5537fe37b76d2a0a38ae76e (accessed Dec 28, 2023).

(207) V  ril, M.; Scemama, A.; Caffarel, M.; Lipparini, F.; Boggio-Pasqua, M.; Jacquemin, D.; Loos, P.-F. QUESTDB: A database of highly accurate excitation energies for the electronic structure community. *Wiley Interdiscip. Rev.: Comput. Mol. Sci.* **2021**, *11*, No. e1517.

(208) Loos, P.-F.; Scemama, A.; Boggio-Pasqua, M.; Jacquemin, D. Mountaineering Strategy to Excited States: Highly Accurate Energies and Benchmarks for Exotic Molecules and Radicals. *J. Chem. Theory Comput.* **2020**, *16*, 3720–3736.

(209) Sherrill, C. D.; Krylov, A. I.; Byrd, E. F. C.; Head-Gordon, M. Energies and analytic gradients for a coupled-cluster doubles model using variational Brueckner orbitals: Application to symmetry breaking in O₄⁺. *J. Chem. Phys.* **1998**, *109*, 4171–4181.

(210) Krylov, A. I.; Sherrill, C. D.; Byrd, E. F. C.; Head-Gordon, M. Size-consistent wave functions for nondynamical correlation energy: The valence active space optimized orbital coupled-cluster doubles model. *J. Chem. Phys.* **1998**, *109*, 10669–10678.

(211) Krylov, A. I.; Sherrill, C. D.; Head-Gordon, M. Excited states theory for optimized orbitals and valence optimized orbitals coupled-cluster doubles models. *J. Chem. Phys.* **2000**, *113*, 6509–6527.

(212) Bozkaya, U.; Turney, J. M.; Yamaguchi, Y.; Schaefer, H. F.; Sherrill, C. D. Quadratically convergent algorithm for orbital optimization in the orbital-optimized coupled-cluster doubles method and in orbital-optimized second-order M  ller-Plesset perturbation theory. *J. Chem. Phys.* **2011**, *135*, 104103.

(213) Saha, B.; Ehara, M.; Nakatsuji, H. Singly and Doubly Excited States of Butadiene, Acrolein, and Glyoxal: Geometries and Electronic Spectra. *J. Chem. Phys.* **2006**, *125*, 014316.

(214) Schapiro, I.; Sivalingam, K.; Neese, F. Assessment of n-Electron Valence State Perturbation Theory for Vertical Excitation Energies. *J. Chem. Theory Comput.* **2013**, *9*, 3567–3580.

(215) Sarkar, R.; Loos, P.-F.; Boggio-Pasqua, M.; Jacquemin, D. Assessing the Performances of CASPT2 and NEVPT2 for Vertical Excitation Energies. *J. Chem. Theory Comput.* **2022**, *18*, 2418–2436.

(216) Boggio-Pasqua, M.; Jacquemin, D.; Loos, P.-F. Benchmarking CASPT3 vertical excitation energies. *J. Chem. Phys.* **2022**, *157*, 014103.

(217) Kozma, B.; Tajti, A.; Demoulin, B.; Izsak, R.; Nooijen, M.; Szalay, P. G. A New Benchmark Set for Excitation Energy of Charge Transfer States: Systematic Investigation of Coupled Cluster Type Methods. *J. Chem. Theory Comput.* **2020**, *16*, 4213–4225.

(218) Loos, P.-F.; Comin, M.; Blase, X.; Jacquemin, D. Reference Energies for Intramolecular Charge-Transfer Excitations. *J. Chem. Theory Comput.* **2021**, *17*, 3666–3686.

(219) Loos, P.-F.; Jacquemin, D. A Mountaineering Strategy to Excited States: Highly Accurate Energies and Benchmarks for Bicyclic Systems. *J. Phys. Chem. A* **2021**, *125*, 10174–10188.